UNIVERSITÀ
DEGLI STUDI
DI TORINO

Department of Molecular Biotechnologies and Health Sciences
PhD in Molecular Medicine

XXXII cycle
2016-2021

"Finding the keys to Liver Fibrosis Therapy: from novel pathogenic mechanisms to vesicles-based approaches"

Tutor
Prof. Fiorella ALTRUDA

Candidate
Marta MANCO

INDICE

ABSTRACT

Progressive liver fibrosis represents a major health issue worldwide for which no effective treatment is available, thus leading to cirrhosis and ultimately to hepatocarcinoma. Hence, there is urgent need to find alternative therapeutic strategies.

In recent years, stem cell-derived Extracellular Vesicles (EVs)-based therapy has been proposed as a feasible and promising alternative approach to liver transplantation in patients with end-stage liver diseases. For this reason, we assessed the therapeutic potential of human liver adult stem cells (HLSCs)-derived EVs in a mouse model of chronic liver disease, namely cholestasis-induced liver fibrosis. Fibrotic mice intravenously received, with three different treatment regimens, EVs or the vehicle. Briefly, in all the experiments, serum biochemistry and gene expression analysis, as well as histological examination of the livers revealed that HLSCs-derived EVs fail to ameliorate liver fibrosis. Biodistribution analysis of fluorescent labeled-EVs showed that EVs are not able to infiltrate into the fibrotic liver. For this reasons, we concluded that HLSCs-EVs did not exhibit therapeutic properties in our cholestasis-induced liver fibrosis mouse model because of their inability to properly reach the fibrotic and damaged liver.

Nevertheless, the development of new therapeutic strategies requires an extensive knowledge of both cellular and molecular mechanisms underlying hepatic fibrogenesis. In the last years, Liver Sinusoidal Endothelial Cells (LSECs) have gained particular attention. LSECs can be distinguished from all the other ECs in our body because of the presence of both “open” (i.e., without diaphragm) fenestrae and a disorganized/incomplete basement membrane. Interestingly, despite their high specialization, LSECs retain a considerable phenotypic and functional plasticity. Nowadays, LSECs dedifferentiation or sinusoidal capillarization (namely the loss of fenestration and deposition of an organized subendothelial basement membrane) is considered a hallmark of liver fibrosis and cirrhosis, as well as it is implicated in the onset and progression of liver fibrosis. This central role in Chronic Liver Diseases (CLDs) makes them an attractive and promising therapeutic target of new strategies that aim at restoring LSECs fenestration and, consequently, at interfering with CLD progression. Importantly, the bioinformatic analysis of a public microarray dataset revealed that the heme exporter *Flvcr1a* is particularly enriched in LSECs, compared to the other tissue-specific ECs. Starting from this important hint, we started questioning about the possible involvement of FLVCR1a in the maintenance of fenestration. To unveil the biological role of the heme exporter FLVCR1a in LSECs, we performed gain- and loss-of-function *in vitro* assays. Briefly, both FLVCR1a-overexpressing and FLVCR1a-silenced cell lines did not exhibit differences in terms of both heme and ROS levels, compared to their respective controls, as well as in terms of cell viability. Then, we measured membrane fluidity, as an indirect parameter of fenestration. The results suggest that FLVCR1a positively regulates membrane fluidity, thus allowing us to speculate that FLVCR1a can positively regulate fenestrae formation and/or maintenance. Mechanistically, we demonstrated that, by modulating FLVCR1a levels, we can affect heme synthesis and, consequently, cholesterol synthesis. This metabolic adaptation could be at the basis of the different membrane cholesterol content and, consequently, of the different membrane fluidity, observed following FLVCR1a levels modulation. Overall, we could speculate that normal LSECs have a different metabolic signature compared to dedifferentiated ones. For this reason, by modulating heme/cholesterol metabolism we could affect LSECs fenestration.

INTRODUCTION

Chronic Liver Disease(s): Epidemiology, Definition and Treatment

Globally, approximately 1.5 billion people had a Chronic Liver Disease (CLD) in 2017, most commonly resulting from Non-Alcoholic Fatty Liver Disease (NAFLD, 60%), Hepatitis B Virus (HBV, 29%), Hepatitis C Virus (HCV, 9%) and Alcohol-related Liver Disease (ALD, 2%)[1]. Based on data from the Global Burden of Disease study, the age-standardized incidence rate of CLDs and cirrhosis, one of its major complications, was 20.7 per 100,000 in 2015, a 13% increase from 2000[1]. Moreover, CLDs account for approximately 2 million deaths each year worldwide. In particular, the major complications of a CLD, namely cirrhosis (1.2 million deaths/year) and hepatocellular carcinoma (790,000 deaths/year), account for 3.5% of all deaths worldwide, thus representing the 11th and 16th cause of death, respectively[2]. However, beyond mortality, high burden of disability and increased health care utilization have been attributed to CLDs and cirrhosis[1]. Overall, these epidemiologic data suggest that, nowadays, CLDs and related complications (i.e., cirrhosis and hepatocellular carcinoma) are one of the major health problems worldwide.

CLDs can be regarded as the result of continuous and repeated insults to the liver. An insult inflicted upon liver cause injury and the consequent activation of a "normal" wound healing response (i.e., fibrogenesis), which involves [1] the activation and recruitment of immune and/or inflammatory cells, [2] the secretion and reorganization of extracellular matrix (ECM) proteins and [3] the hepatic regeneration[3]. Consistently, repair of damaged tissues is a fundamental biological process that allows the ordered replacement of dead or damaged cells after injury, a mechanism that is critically important for survival[4]. However, although initially beneficial, the healing process becomes pathogenic if the harmful stimulus is not promptly removed, thus leading to the progressive substitution of liver parenchyma with excessive ECM deposits (i.e., fibrosis)[4]. Liver fibrosis over time (inevitably) causes the disruption of liver architecture and, ultimately, the loss of its normal functionality. For this reason, fibrosis is considered the mainstay for untreated CLDs and the "*condicio sine qua non*" for the subsequent onset of its major complications, namely cirrhosis and hepatocellular carcinoma[5,6] (Fig. 1).

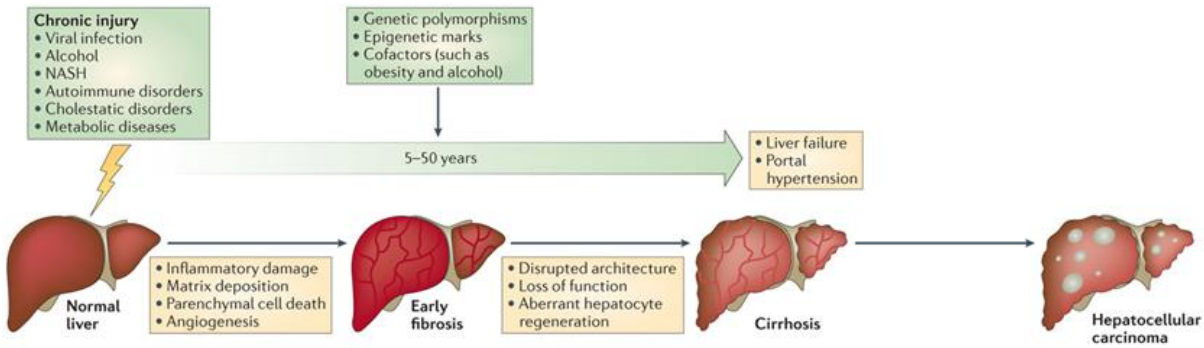

Figure 1. Natural history of a CLD. Hepatic fibrosis is the wound-healing response of the liver to many causes of chronic injury (e.g., viral infection, alcohol and cholestatic disorders). Regardless of the underlying cause, iterative injury causes inflammatory damage, matrix deposition, parenchymal cell death and angiogenesis leading to progressive fibrosis. The scar matrix typically accumulates very slowly (the median time to cirrhosis in chronic hepatitis C is 30 years) but once cirrhosis is established the potential for reversing this process is decreased and complications, such as portal hypertension, liver failure and hepatocellular carcinoma, develop. (*Figure adapted from*[6])

Nowadays, several aetiologies underlying a CLD have been recognized, including for example Cholestasis. Cholestatic liver diseases are caused by an impaired flow of bile from the liver to the duodenum. The major components of bile are bile salts, which are strong detergents, and other endogenous and potentially toxic compunds (e.g., bilirubin) resulting from the clearance function of the liver. As a consequence, the accumulation of bile compounds causes unspecific cellular damage, thus initiating a well-coordinated cascade of inflammatory and fibrogenic events in the liver[7,8]. A longitudinal study, performed on a cholestatic mouse model, has allowed the authors to resolve these inflammatory and fibrogenic events[8]. However, of interest, the natural history of CLDs is marked by similar cellular and molecular events, regardless of the underlying cause. Firstly, the exposure to a toxic stimulus (e.g bile compounds) triggers the necrosis of hepatocytes and cholangiocytes, thus initianting a regenerative and inflammatory response. In particular, hepatocytes and cholangiocytes start proliferating and macrophages, once activated, start releasing pro-inflammatory cytokines. However, this substained pro-inflammatory environment, due to a substained exposure to the toxic stimulus, blocks hepatocytes proliferation, while triggering [1] the activation of stellate cells, which are the main producers of ECM, and [2] the so-called "Ductular Reaction" (DR). This phenomenum involves the activation and proliferation of oval cells (i.e., bipotent progenitor cells resident in the adult liver), as well as their "differentiation" into the so-called reactive cholangiocytes[9,10]. The latters contribute to the amplification of the pro-inflammatory and pro-fibrogenic processes, by stimulating and maintaining over time the inflammatory response and the activation of Hepatic Stellate Cells (HSCs)[10]. Overall, these steps continue to perpetuate over time, thus leading to the massive and progressive deposition of ECM[8] (Fig. 2).

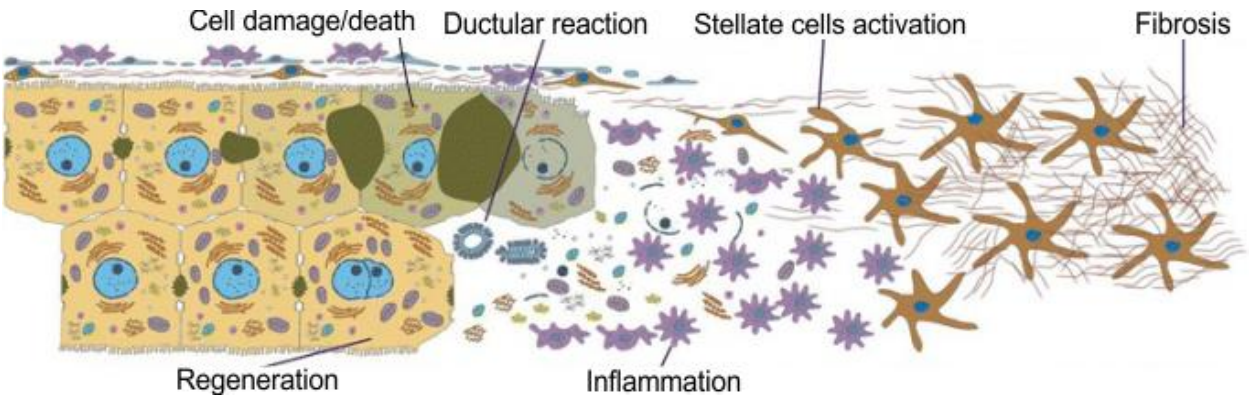

Figure 2. Outline of the disease process. The exposure to a toxic stimulus triggers the unspecific cellular damage/death, thus generating a pro-inflammatory and pro-fibrotic environment. The latter, in turn, limits the hepatic regeneration, whereas exhacerbates the activation of HSCs and, consequently, the progressive deposition of ECM in liver parenchyma. The ductular reaction plays a central role in this depicted disease process, thus boosting and maintaining over time inflammation and HSCs activation. (*Figure adapted from[8]*)

Nevertheless, it is further noteworthy that the fibrogenic process is extremely dynamic and even reversible. In fact, if the cause of fibrosis is eliminated, resolution (i.e., complete reversal to near-normal liver achitecture) of early hepatic fibrosis can occur. As a consequence, nowadays, the best anti-fibrotic therapy is the elimination of the underlying harmful stimulus. However, even though there is a general consensus that, if the underlying cause is eliminated, liver fibrosis in humans is potentially reversible, scepticism prevails on the concept that also cirrhosis can be truly reversed[11]. In this sense, the removal of the harmful stimulus is not

sufficient anymore and these patients need other anti-fibrotic therapies. However, currently the only available treatment for liver failure is liver transplantation. As mentioned before, the incidence of CLDs worldwide is very high and increases over time. For this reason, despite being the second most common solid organ transplantation, yet less than 10% of global transplantation need are met at current rates[2].

Overall, CLDs and cirrhosis represent a major world health problem due to the high incidence and, most importantly, due to the lack of therapeutic treatments other than liver transplantation. This strongly highlights the urgent need to find alternative approaches.

Stem Cell (and derivatives) Therapy in Liver Failure

In recent years, stem cell therapy has been proposed as a promising alternative approach to liver transplantation in patients with end-stage liver diseases (e.g., with liver failure). Consistently, several studies have been performed to evaluate both the safety and the efficacy of stem cell therapy in these patients[12]. However, as reported in this recent systematic review[12], we are still too far from its clinical applicability, mostly because of the lack of a standardized method. Likewise, from the compilation and analysis of the various studies, emerged variabilities in terms of the type of cells (e.g., Bone marrow-derived Mesenchymal Stem Cells, BM-MSCs, and Peripheral Blood-derived $CD34^+$ or $CD133^+$ cells, PB-$CD34^+$ cells or PB-$CD34^+$ cells, respectively), the dose, the route and the outcome measures to assess the success of therapy[12].
Nevertheless, it is further noteworthy that the clinical applicability of stem cell therapy in liver failure could be also hampered by other long-term drawbacks. Consistently, the majority of pre-clinical and clinical studies analyzed the results of treatment in few months or years[12,13]. Stem cells can be regarded as undifferentiated cells that replicate indefinitely (i.e., self-renewal capability) and that have the potential to develop into many different specialized cells (i.e., differentiation capability). It is precisely from these two intrinsic capabilities that stem cell therapy-related long-term drawbacks arise. For example, tumor cells actually behave very much like stem cells (they divide indefinitely and tend to be undifferentiated). Consistently, concerns have been raised about the potential for tumors to develop from transplanted stem cells[14–16]. Moreover, it has been shown that transplanted stem cells, after having engrafted the damaged site, can undergo a process of maldifferentiation[17,18]. Overall, although stem cells transplantation might provide effective treatments for liver failure[12,13,19], in the last years some concerns have been raised over its safety.

How can we harness the benefits of stem cell therapy, while overcoming its potential long-term drawbacks?

Initially the regenerative paradigm in stem cell therapy was based on the assumption that stem cells could play a critical role in tissue repair by means of their plasticity in giving rise to new functional differentiated cells (e.g., hepatocytes). However, the results of a large number of studies have pointed out a recent paradigm shift. Consistently, the mechanisms underlying the benefits achieved by transplanting stem cells appear to relate primarily to their paracrine modulatory effect, rather than direct replacement of damaged/lost cells through their direct differentiation[20]. It has been proposed the “Teamwork hypothesis”, through which exists a

synergistic crosstalk between the transplanted stem cells and the resident tissue cells. It is indeed more plausible that exogenous stem cells release a variety of crucial factors that can instruct resident cells, thus boosting the "*in situ*" regenerative and repair processes.

Over the last years, the researchers have looked at these crucial paracrine factors, by pinpointing out a pivotal role of (exogeneous) stem cells-released Extracellular Vesicles (EVs) in tissue repair[21–25].

Stem cells as a source of EVs

Both prokaryotic and eukaryotic cells communicate and exchange information by employing different cell-cell contact mechanisms involving secreted peptides, bioactive lipids, nucleotides, as well as interactions mediated by sets of specialized adhesion molecules and their ligands[25]. However, growing attention is now being focused on cell-to-cell communication that involves the above-mentioned EVs[21–25], a mechanism that for many years has been largely overlooked. Mounting evidence demonstrates that [1] several cell types employed in regenerative medicine for therapy of damaged organs, such as Hematopoietic Stem Progenitor Cells (HSPCs), Adipose tissue Stem Cells (ASCs), as well as Cardiac Stem Cells (CSCs), are a rich source of EVs and that [2] they repair a damaged tissue, thus improving its functionality, through the release of such EVs[18,26–30].

It was already acknowledged that EVs are secreted or shed by healthy and not dying cells, are much smaller in size than apoptotic bodies and do not contain fragments of nuclei loaded with nuclear DNA, which is a common feature of apoptotic bodies. However, there is no doubt that the biological significance of EVs has for many years been largely overlooked and that EVs have been regarded, like apoptotic bodies, as mere cellular fragments or debris. Over the last years, this stance has dramatically changed with the recognition of EVs as carriers of biologically active molecules that can traffic to local or distant targets and execute defined biological functions. EVs can indeed be regarded as double-layer phospholipid membrane vesicles carrying a battery of bioactive cargo of soluble and membrane-bound proteins, lipids, metabolites, DNA, and RNA (mRNA, miRNAs and other small regulatory RNAs), thus reflecting the content of their cell of origin[24]. However, as depicted in the Fig. 3, EVs are a heterogeneous population. To simplify, based on the current state of the knowledge of their biogenesis, as well as on their size, they have been classified into two subgroups, namely [1] exosomes and [2] microvesicles. In particular, [1] exosomes are the smallest vesicles (30-150 nm) and are formed by the interior budding of endosomal membranes to form large multivesicular bodies (MVBs), while [2] microvesicles are the largest ones (100-1000 nm) and are produced by budding from the plasma membrane[24].

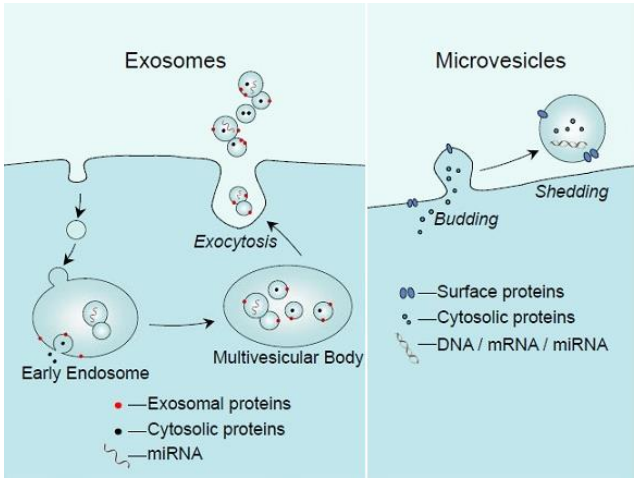

Figure 3. Exosomes *versus* Microvesicles: size and biogenesis. Exosomes are the smallest vesicles (30-150 nm) released by the fusion of MVBs, containing intraluminal vesicles, with the plasma membrane. Microvesicles are vesicular structures (100-1000 nm) shed by outward blebbing of the plasma membrane. *(Figure adapted from[145])*

Taking together, it has been suggested that the EVs-mediated paracrine effects make major contributions in the most of the currently reported positive results in both pre-clinical and clinical studies employing stem cells[18,26–30]. As a consequence, all these findings have laid the foundation for a EVs-based cell-free therapy, thus overcoming the potential long-term stem cell-related drawbacks. However, despite the recent important advances, as reviewed elsewhere[31], there are still some unsolved mysteries and technical hurdles that challenge the field of EVs research and their imminent use into the routine clinical practice.

Human adult Liver Stem Cells (HLSCs): a new promising EVs source

During the last years, several studies on both animals and humans have been performed, by testing the efficacy of several stem cell types and related EVs. Among them, it is getting more and more attention over time a specific adult stem cell population, namely Human Liver Stem Cells (HLSCs)[19].

Evidences from several studies for long time have suggested the presence of resident stem cells in the human normal adult liver, besides the already well-known oval cells (also known as Liver Progenitor Cells, LPCs)[32,33]. However, this stemness properties-harbouring cell population has been unknown to the scientific community until the pioneering work of Herrera M.B. *et al.*, published in 2006[34]. The authors isolated from human liver biopsy a population of stem cells, currently known as HLSCs, which exhibited a high proliferative capacity under very stringent culture conditions (in which mature hepatocytes undergo cell death). Subsequently, HLSCs were deeply characterized from a molecular and morphological point of view. This cell population express many surface markers in common with MSCs (i.e., CD73, CD29, CD105, CD90 and CD44), various stem cell and embryonic markers (i.e., Nanog, Oct3/4, Sox2, Musashi, SSEA4, and Pax2) and markers specific to hepatic cells (Albumin, CK8, and CK18)[34]. Moreover, the morphology and the absence of CD34, c-kit and CK19 indicated that HLSCs represent a population of liver precursors different from oval cells[34]. Similarly, the authors characterized HLSCs also from a "functional" point of view, thus showing that the above-mentioned HLSCs fulfil both criteria for stem cell definition (i.e., the capacity for self-renewal and multipotent differentiation)[34–36]. Overall, HLSCs can be regarded as multipotent stem cells with a partial committment to the hepatic lineage, thus providing the basis for their use cell therapy strategies in patients with liver diseases.

Over the last years, a variety of pre-clinical studies involving animal models of severe liver diseases (e.g., acute liver injury and Crigler-Najjar Syndrome type I) has demonstrated the propensity of HLSCs to engraft injured livers and to improve liver morphology and liver function[34,37,38]. These promising "efficacy data" have been recently supported and strengthen by "safety data" obtained from a clinical trial on two infants with Inherited Neonatal-Onset Hyperammonemia[39]. None of the patients experienced infections, hyperammonemia decompensation or other adverse events during the whole observation period (19 and 11 months, respectively). Moreover, no Donor Specific Antibodies (DSA) against HLSCs were detected. Therefore, these findings suggest that the percutaneous intrahepatic administration of HLSCs is safe (at least until 19 months) in newborns with inherited neonatal-onset hyperammonemia[39]. Subsequently, strongly motivated by these promising results, the same group (Camussi G., Unito) evaluated whether HLSCs may offer an alternative option for the treatment of end-stage liver diseases. Consistently, Bruno S. *et al.* recently demonstrated the therapeutical potential of HLSCs in a Non-Alcoholic SteatoHepatitis (NASH) mouse model. In fact, the treatment with HLSCs exhibited both anti-fibrotic and anti-inflammatory effects[40]. Of interest, the majority of the human cells detected in the liver parenchyma of fibrotic mice lacked the expression of specific markers of hepatic differentiation, thus suggesting that [1] HLSCs persisted in an undifferentiated state and that [2] the anti-fibrotic and anti-inflammatory effects do not rely on the differentiation of HLSCs into mature hepatocytes[40]. For this reason, taking together, it is more plausible that the healing properties of HLSCs in a model of CLD are due to paracrine mechanisms, rather than the replacement of damaged/lost hepatocytes. This speculation is perfectly in concordance with the previously discussed “Teamwork hypothesis” underlying the therapeutic stem cell transplantation-related effects. Considering the pivotal role of EVs in cell-to-cell communication, a question arose spontaneously and naturally:

Do HLSCs exert anti-inflammatory and anti-fibrotic effects through the release of EVs?

Taking together, the results obtained over the last years by Camussi’s group pinpoint out a potential pro-regenerative and anti-fibrotic properties of HLSCs-derived EVs, thus encouraging their utilization in CLDs animal models.

Liver Sinusoidal Endothelial Cells as a novel therapeutic target in Liver Failure

Nowadays, (stem cell-derived) EVs-based therapy is considered a feasible and promising alternative to liver transplantation. However, before moving to the routine clinical practice, many efforts still need to be made in the future, thus assessing the efficacy and the safety of this approach. Nevertheless, the development of new therapeutic strategies requires an extensive knowledge of both cellular and molecular mechanisms underlying hepatic fibrogenesis. Therefore, there is an urgent need to deeper elucidate these mechanisms. For long time, it has been widely recognized that HSCs are one of the most important fibrogenic cells in the liver[41,42]. These cells undergo a transformation during injury, termed “activation”. The activation process is complex, but one of its most prominent features is the synthesis of large amounts of ECM, resulting in the deposition of scar or fibrous tissue. For this reason, over the past 30 years, great advances in the field of stellate cells have been made, thus opening new therapeutic windows[41,42]. However, yet most of the therapies are still in pre-clinical or

early clinical evaluation stages. It is further noteworthy that, as previously discussed, the fibrogenic process is extremely complex and involves the cross-talk of several liver cell populations. Of interest, in the last years Liver Sinusoidal Endothelial Cells (LSECs) have gained particular attention, because of their central role in liver homeostasis maintenance and in triggering liver fibrosis.

To encounter each organ specific physiological function, microvascular Endothelial Cells (ECs) undergo a process of specialization and differentiation (i.e., vascular organotypicity)[43]. In fact, in our body exist three major types of capillaries with a different grade of permeability and molecular transport (from the lowest to the highest): continuous, fenestrated and sinusoidal. LSECs, lining the hepatic sinusoids, are liver-specifically differentiated microvascular ECs and represent about 70% of Non-Parenchymal Cells (NPCs). LSECs, despite falling into the category of sinusoidal capillaries with spleen and bone marrow ECs, can be regarded as unique ECs in our body because of the presence of open (non-diaphragmed) fenestrae and a disorganized basement membrane. Thanks to the pioneering work of Wisse E. in 1970[44] and subsequent reports of Widmann J.J.[45] and Ogawa K.[46], nowadays LSECs fenestrae can be regarded as transcellular open pores of approximately 100-150 nm in size clustered in groups, the so-called sieve plates, thus occupying around 6-8% of the endothelial surface. Based on morphological assessment and functional evidences[47], it has been postulated that, differently from all other ECs, LSECs act as a sieve, by filtering in a "passive and size-selective manner" virus, solutes and particles (e.g., chylomicron remnants) smaller than fenestrae diameter from and to the space of Disse[48–51]. Consistently, LSECs do not represent a barrier for macromolecule transport as ECs in other organs but allow a bidirectional "open" solute exchange between blood and hepatocytes, thus encountering the physiological functions of the liver.
Interestingly, despite their high specialization, LSECs retain a considerable phenotypic and functional plasticity. In fact, LSECs fenestrae are dynamic structures, meaning that their number and diameter can change over time in the hepatic vascular beds upon external stimuli[47]. Loss of fenestration and deposition of an organized subendothelial basement membrane is called "capillarization"[47,52] (Fig. 4). Nowadays, LSECs dedifferentiation or sinusoidal capillarization is considered a hallmark of liver fibrosis and cirrhosis, regardless of the underlying disease cause[53–57]. For example, Miyao M. *et al.* showed that Scanning Electron Microscopy (SEM) analysis of livers derived from mice fed two different fibrogenic diets (DDC-supplemented diet and CDAA diet) revealed, already at very early time points, sinusoidal capillarization[58,59].

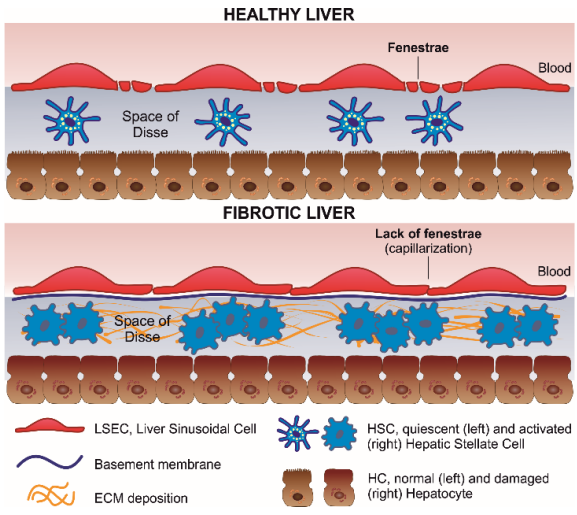

Figure 4. Schematic representation of structural differences between normal and cirrhotic sinusoidal milieu. In normal liver (top), the presence of open fenestrae and the lack of basement membran allow a bidirectional "open" exchange between blood and the space of Disse, where reside quiescent HSCs. In the fibrotic liver (bottom), there is the deposition of an organized basement membrane along the sinusoids, the loss of LSECs fenestrae and the activation of HSCs, which in turn cause excessive collagen deposition whithin the space of Disse. *(Figure adapted from*[146])

Can dedifferentiated LSECs be regarded as “active players” or “passive bystanders” in CLD pathogenesis?

ECs have long been considered as passive cells delimiting blood vessels. However, during the last years several studies have shown that ECs are, instead, actively involved in organ development, regeneration and homeostasis maintenance[43,60–62]. Furthermore, it is becoming increasingly clear that, at the basis of many chronic and life-threatening diseases (e.g., metabolic disorders, atherosclerosis and cancer), there is a vascular dysfunction, emphasizing once again the importance of ECs in ensuring a proper organ and, consequently, body physiological function[63]. To this regard, it has been postulated that dedifferentiated LSECs (i.e., without fenestrae) in the hepatic sinusoids are one of the major determinants of liver fibrosis, rather than simple “passive bystanders”. Consistently, several studies performed on both human and animal models demonstrated that normal differentiated LSECs act as gatekeepers of fibrogenesis by maintaining the quiescence of HSCs[64–67], thus implying that LSECs capillarization precedes the onset of liver fibrosis[66,68,69]. Moreover, it has been shown that LSECs directly contribute to [1] ECM deposition through the production of collagen and fibronectin[70,71] and to [2] heighten inflammatory milieu, as well as alter intrahepatic immunity[72–74]. Lastly, LSECs play a pivotal role not only in the early stages of CLD but also in the later ones. In fact, it has been demonstrated that dedifferentiated LSECs promote portal hypertension[75–77]. Overall, LSECs are implicated in the maintenance of liver homeostasis, as well as in the onset and progression of liver fibrosis. This central role in CLDs makes them an attractive and promising therapeutic target.
However, despite the first observation of LSECs fenestration dates to 1970 and their pivotal role in CLD pathogenesis has been widely recognized over the years, the molecular and structural mechanisms underlying the formation, maintenance and dynamic regulation of LSECs fenestrae are still elusive. Therefore, further works will be indispensable to deeper understand these mechanisms, thus opening new therapeutic windows aiming at restoring LSECs fenestration and, consequently, at interfering with CLD progression and the onset of its complications, such as portal hypertension[78].

FLVCR1a and its vital role in ECs during embryo development

As previously stated, it is imperative to deeper unravel the major molecular determinants of LSEC fenestration, thus highlighting new “druggable” molecular pathways.
Over the last years, it has been demonstrated that normal ECs and dysfunctional/diseased ECs exhibit a different metabolic profile, thus suggesting that metabolism could be a major determinat of ECs biology and, consequently, of the whole pathological process[79]. As a consequence, novel “EC metabolism-centric” therapeutic avenues are recently proposed. Besides the most common studied metabolic pathways (e.g., glycolysis and glutaminolysis), heme metabolism, which has been overlooked for long time, is currently getting more and more attention and seems to be tighly connected to the other pathways[80–83]. However, so far the molecular profile of differentiated and dedifferentiated LSECs has never been extensively explored[84].

Heme, a complex of iron with protoporphyrin IX, is ubiquitous in aerobic cells and has pleiotropic functions. In fact, it serves as co-factor of a large array of proteins (i.e., hemoproteins) involved in fundamental biological processes, including oxidative metabolism, oxygen storage and transport, signal transduction and drug metabolism[85]. In addition, heme is important for systemic iron homeostasis in mammals[85]. Of interest, the role of heme in other fundamental cell processes (e.g., regulation of microRNA processing[86], circadian rhythm[87] and ion-channel functions[88]) has been described. These observations seem to argue for a physiological role for a "free" or "uncommitted" heme pool (i.e., intracellular heme that is not a component of hemoproteins). However, free heme is lipophilic and toxic to cells, promoting lipid peroxidation[89,90] and the production of Reactive Oxygen Species (ROS)[91], thus resulting in membrane injury and cell apoptosis[90]. Therefore, both from the viewpoint of its toxicity and its regulatory function, the intracellular levels of free heme must be tightly controlled (Fig. 5). Control of intracellular heme levels was previously thought to occur through a balance among its biosynthesis, utilization by hemoproteins and catabolism by Heme Oxygenases (HO) (predominantly by the heme-inducible HO-1)[92]. However, studies describing transporters of heme and heme synthesis intermediates indicate further layers of complexity in heme homeostasis[93].

Recently, heme export through the cell surface transporter Feline Leukemia Virus subgroup C Receptor 1a (FLVCR1a) has been proposed as an additional control step to prevent the intracellular accumulation of heme[85,94].

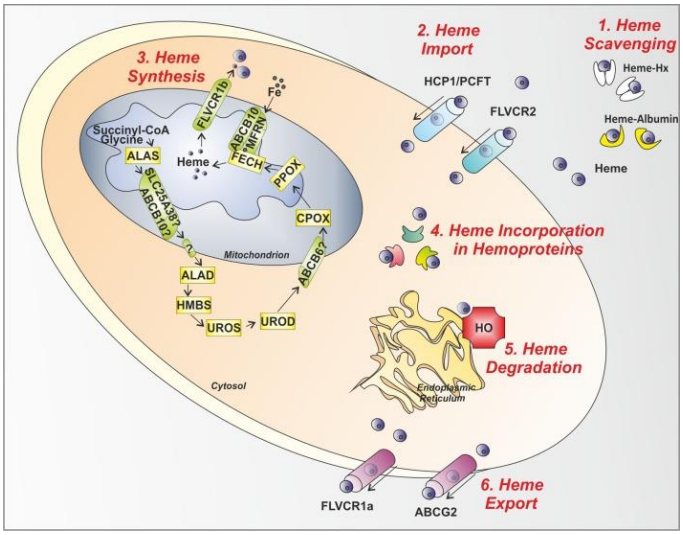

Figure 5. Control steps in heme metabolism. (1) Heme scavenging. (2) Heme Import. (3) Heme Synthesis: In the mitochondrion and cytosol, the heme biosynthetic enzymes, starting from succinyl-CoA and glycine, give rise to heme. After synthesis, heme is exported out of the mitochondrion to the cytosol by the mitochondrial heme exporter FLVCR1b. (4) Heme Incorporation in Hemoproteins: once released in the cytosol, heme is inserted in apo-hemoproteins to allow the formation of functional hemoproteins. (5) Heme Degradation: In the endoplasmic reticulum, the heme degrading enzyme HO is responsible for heme degradation into iron (Fe), carbon monoxide and biliverdin. (6) Heme Export: The heme exporters FLVCR1a and ABCG2 regulate heme export out of the cell across the plasma membrane. *(Figure from[89])*

However, it is further noteworthy that *FLVCR1* gene, also known as *MFSD7B*, actually encodes for two different proteins, FLVCR1a and FLVCR1b, expressed at the plasma membrane and on the mitochondria, respectively[95]. FLVCR1a, in which we are particularly interested in, belongs to the SLC49 family of the Major Facilitator Superfamily (MFS) of transporters with 12 hydrophobic transmembrane domains[85,96]. FLVCR1b is a shorter protein with only 6 transmembrane domains, supposed to homodimerize to form a functional transporter[96]. To simplify, it has been demonstrated a crucial role for FLVCR1b in the last step of heme biosynthetic pathway (i.e., heme export from the mitochondria toward cytosol)[96]. On the other hand, FLVCR1a exerts its heme export activity at the plasma membrane, thus avoiding

intracellular heme loading and, consequently, heme-related toxicity[94,97]. The term "FLVCR1" derived from the observation that domestic cats infected with Feline Leukemia Virus subgroup C (FeLV-C), by binding a specific cell surface receptor (currently known as FLVCR1) on Colony-Forming Unit-Erythroid progenitor (CFU-E)/pro-erythroblast stage, exhibited a severe aplastic anemia[85]. Therefore, FLVCR1 was identified in 1999 as a receptor that appeared to be critical for the development of erythroid progenitors[98,99]. However, over the years, it has been shown that FLVCR1a is ubiquitously expressed, thus arguing for its involvement in other biological processes, besides erythropoiesis. Consistently, several studies performed on tissue-specific conditional Knock-Out (KO) mice or patient-derived cells have unveiled these multiple roles. For example, it has been shown that the loss of FLVCR1a in hepatocytes negatively affects the expression and activity of cytochrome P450, thus highlighting important implications for drug metabolism[95]. Moreover, a subsequent work revealed a crucial role for FLVCR1a in maintaining intestinal mucosa homeostasis in both physiologic and pathologic (i.e., ulcerative colitis) conditions[100]. However, despite these findings obtained in mice are suggesting a role of this exporter in both liver and intestine, so far mutations in *FLVCR1a* gene have been found only in patients with neurodegenerative disorders (i.e., Posterior Column Ataxia, Retinitis Pigmentosa and Hereditary Sensory and Autonomic Neuropathy). Consistently, multiple studies have demonstrated that *FLVCR1a* mutations trigger the dysregulation of heme homeostasis and, consequently, the degeneration of specific neuronal cell populations[101–104].

What about FLVCR1a role in the endothelial compartment?

In 2012 Chiabrando D. *et al.* demonstrated that the (total) *Flvcr1a*$^{-/-}$ embryos (but still expressing FLVCR1b) died between E14.5 and birth[96]. It has been hypothesized that the embryonic death of *Flvcr1a*$^{-/-}$ mice was likely due to multifocal and extended hemorrhages, associated with subcutaneous edema. To investigate the overall vascular architecture, whole-mount CD31 immunostaining was performed on E11.5 *Flvcr1a*$^{-/-}$ embryos[96]. *Flvcr1a*$^{-/-}$ embryos showed reduced vasculature extension and complexity compared to controls. This was particularly evident in the primordial limbs and tail, where vessels did not form properly and branching was severely compromised. However, in addition to vascular defects, *Flvcr1a*$^{-/-}$ embryos showed skeletal abnormalities similar to those reported in mice lacking both *Flvcr1* isoforms[97]. These results highlighted an important and vital role of the specific isoform FLVCR1a in the vascular compartment. Subsequently, to further strengthen these findings, endothelial-specific *Flvcr1a*$^{-/-}$ mice were generated, thus providing once again evidence that heme homeostasis in ECs controls the angiogenic process[80]. In particular, Petrillo S. *et al.* showed that FLVCR1a loss in ECs leads to an expansion of the intracellular heme pool and promotes cell death by paraptosis, a specific type of programmed cell death[80]. Paraptosis of *Flvcr1a*$^{-/-}$ ECs in mouse embryo prevented the formation of a well-defined and functional microvascular network, thus leading to extensive hemorrhages and embryonic lethality[80] (Fig. 6). Of interest, the analysis of embryonic organs, with both X-ray micro-computed tomography and histologic examination, did not reveal the presence of evident malformations in endothelial-specific *Flvcr1a*$^{-/-}$ embryos compared to controls, except for the fetal liver that was smaller in *Flvcr1a* eKO embryos compared to controls[80] (Fig. 6).

Taking together, these results, as the previous ones on total KO, stricktly suggest that FLVCR1a is extremely important in ECs, thus regulating their homeostasis and their angiogenic functions

during embryonic development[80,96]. Overall, to deeper unravel the physiological role of this heme exporter in the vascular compartment, it could be interesting to analyze the role of FLVCR1a also in quiescent (not angiogenic) ECs, namely in adult mice, with a particular attention to liver and LSECs.

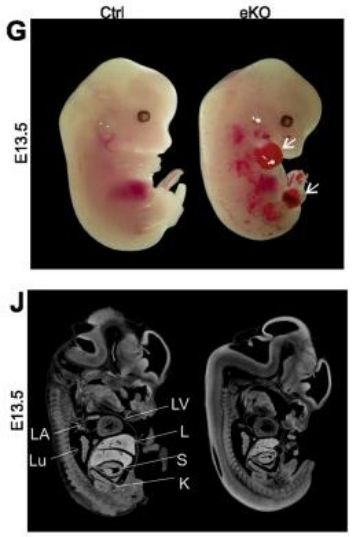

Figure 6. Macroscopic phenotype of Control and eKO embryos. [G] Representative picture of E13.5 control and *Flvcr1a* eKO embryos with undeveloped limbs and intraembryonic hemorrhages (white arrows). [J] X-ray micro-computed tomography analysis on E13.5 embryos showing the internal organs morphology. Differently from the other organs that appeared normal, liver (L) is smaller in *Flvcr1a* eKO embryos, compared to the control (Ctrl) ones. *(Figure adapted from[80])*

AIM(S)

CLDs and cirrhosis represent a major world health problem due to the high incidence and, most importantly, due to the lack of therapeutic treatments other than liver transplantation. This strongly highlights the urgent need to find alternative approaches. Over the years, several efforts have been made to open new therapeutic avenues.

For example, (stem cell-derived) EVs-based therapy is currently considered a feasible and promising alternative to liver transplantation. As previously discussed, the results obtained over the last years by Camussi's group on HLSCs pinpoint out a potential pro-regenerative and anti-fibrotic properties of their EVs. For this reason, in collaboration with Prof. Camussi G. and other Companies in Piedmont, we decided to assess the therapeutic potential of HLSCs-derived EVs in a mouse model of CLD, namely Cholestasis-induced Liver Fibrosis.

However, another branch of CLDs research is currently working on elucidating the cellular and molecular mechanisms underlying hepatic fibrogenesis. A deeper knowledge of these mechanisms is indeed crucial to identify new "druggable" targets and/or pathways. In the last years, LSECs have gained particular attention, because of their central role in liver homeostasis maintenance and in triggering liver fibrosis. Based on the encouraging data about the negative impact of FLVCR1a loss and heme dysregulation in ECs on microvascular network formation during embryonic development, in collaboration with Prof. Tolosano E., we decided to dissect its role in quiescent adult ECs and specifically in LSECs.

To summarize, motivated by the urgent need to find therapeutic alternative to liver transplantation, during my PhD I worked on two different projects:

- **"TRANSLATIONAL/APPLIED" APPROACH**:
  Evaluate the (potential) therapeutic effects of HLSCs-derived EVs in an immunodeficient mouse model of Cholestasis-induced Liver Fibrosis;
- **"BASIC" APPROACH**:
  Unveil the biological role of FLVCR1a and heme metabolism in LSECs in an attempt to deeper elucidate the molecular mechanisms underlying the sinusoidal capillarization in liver fibrosis and, hopefully, to open new therapeutic windows.

RESULTS

Translational/Applied Approach

HLSCs-derived EVs do not display any beneficial effects on Cholestasis-induced Liver Fibrosis, due to their inability to reach the damaged Liver

Characterization of Cholestasis-induced Liver Fibrosis natural history in immunocompromised mice

A xenobiotic-induced liver fibrosis mouse model, partially resembling human cholestatic liver diseases (e.g., Primary Sclerosing Cholangitis and Primary Biliary Cirrhosis), has been previously developed by feeding multiple strains of immunocompetent mice with 0,1% DDC (3,5-Diethoxycarbonyl-1,4-DihydroCollidine)-supplemented diet[105]. As previuosly mentioned, the project involves the administration of human cell-derived EVs. Therefore, to avoid the activation of immune responses and the consequent clearance of EVs, we used NOD Scid Gamma (NSG) immunocompromised mice. However, so far, the DDC-induced cholestatic and fibrotic phenotype has never been assessed in immunocompromised mice. For this reason, we have firstly characterized the natural history of cholestasis-induced liver fibrosis in NSG mice, by designing a longitudinal study. In particular, the experimental workflow consisted in [1] feeding male 6-8 weeks old NSG mice with DDC-supplemented diet (Experimental mice), [2] sacrificing them at different time points (4, 6, 8, 10, 12, 14 and 16 weeks) and, finally, [3] comparing them to Control mice, fed with standard diet (Fig. 7, A). The control mice, to exclude age-related changes, have been sacrified, together with the experimental mice, at three different time points (8, 12 and 16 weeks). To widely characterize the liver status and to assess the progression of cholestasis and fibrosis, we conducted several analysis on both sera and livers[106] (Fig. 7, B).

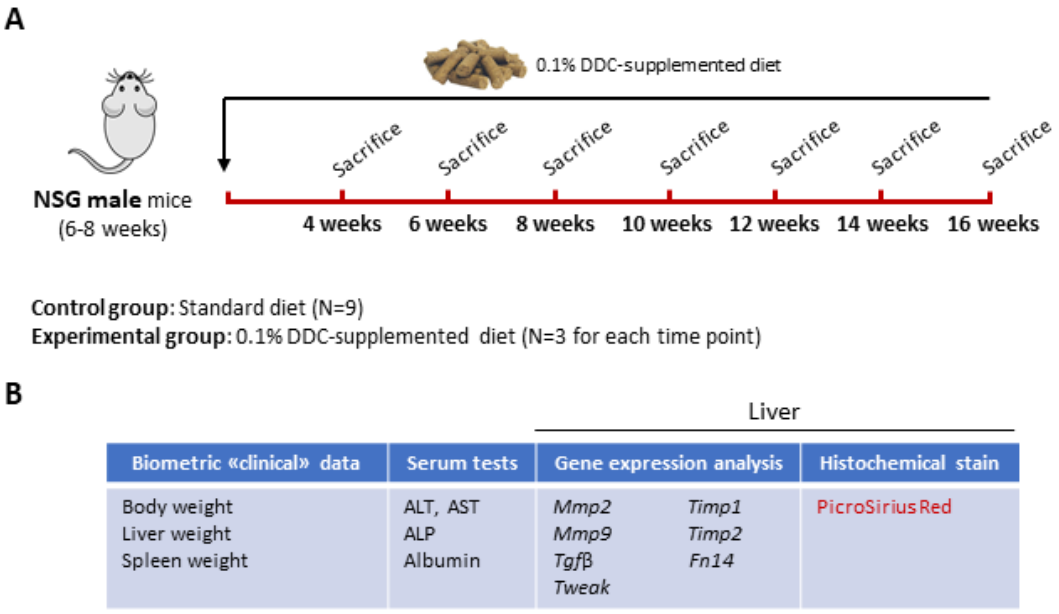

Figure 7. Standardized work-up of Cholestasis-induced Liver Fibrosis mouse model. [A] To assess the natural history of CLD in NSG mice, we sacrified experimental mice at different time points (4, 6, 8, 10, 12, 14 and 16 weeks) of DDC intoxication and we compared them to standard diet-fed mice (control group). **[B]** Body, liver and spleen weight were recorded and sera and livers were collected to measure serum parameters levels, to analyze the expression of pro-fibrotic genes and to assess collagen deposition (histologic examination).

Biometric "clinical" data

Body, liver and spleen weight were recorded upon harvesting, in order to follow the appearance of hepatomegaly and splenomegaly (Fig. 7, B). Hepatomegaly is an indicator of liver damage and attempt to regenerate (hyperplasia and hypetrophy), while splenomegaly is an indicator of portal hypertension, which tipically occurs in the advanced stages of a CLD.

From a macroscopic examination, the age-matched DDC-fed mice showed at all the selected three time points (8, 12 and 16 weeks) a reduced body weight, hepatomegaly and splenomegaly, compared to control mice (Table 1). These results suggest that DDC feeding induces a substantial liver damage, as well as portal hypertension.

	Body Weight (g)	Liver Weight (g)	Spleen Weight (g)	L/B Ratio (%)	S/B Ratio (%)
Control 8w	33,7 ± 1,00	1,87 ± 0,10	0,038 ± 0,005	5,59 ± 0,23	0,11 ± 0,02
8 weeks	*26,05 ± 1,52***	2,73 ± 0,22	0,051 ± 0,007	*10,46 ± 0,34****	*0,20 ± 0,02***
Control 12w	35,05 ± 2,78	1,88 ± 0,25	0,037 ± 0,003	5,36 ± 0,29	0,11 ± 0,01
12 weeks	*26,52 ± 3,08**	3,20 ± 0,55	0,052 ± 0,009	*12,03 ± 0,84****	*0,19 ± 0,01**
Control 16w	35,72 ± 2,37	2,05 ± 0,17	0,040 ± 0,010	5,74 ± 0,54	0,11 ± 0,02
16 weeks	*27,79 ± 0,58***	3,71 ± 0,17	0,063 ± 0,006	*13,34 ± 0,63****	*0,23 ± 0,02***

Table 1. Biometric "clinical" data. Body, Liver and Spleen weights were recorded upon harvesting and are expressed as grams (g). Liver/Body (L/B) weight ratio and Spleen/Body (S/B) weight ratio, expressed as percentage (%), are indexes of hepatomegaly and splenomegaly, respectively. Age-matched control mice were used as reference at each time point (8, 12, 16 weeks). Data shown represent mean ± SD (N=3 for each group). Statistically significant differences (Body weight, L/B and S/B) were evaluated using unpaired t-tests (*p<0.05, **p<0.01, ***p<0.001).

Serum tests

Regarding serum biochemical analysis, we measured the levels of [1] both transaminases (ALT and AST), as indicators of hepatocyte injury, [2] alkaline phosphatase (ALP), as indicator of cholestasis and [3] albumin, as indicator of hepatic function (Fig. 7, B).

Firstly, in control mice, AST, ALT, ALP and albumin levels were perfectly in concordance with their "physiological" range, reported by Charles River (Fig. 8, C), and did not show any significant age-related differences. For this reason, concerning serum tests, as well as gene expression analysis and histologic examination, we pulled all the control mice in one group. Moreover, the above-mentioned biometric data were accompanied by a continuous increase in serum AST and ALT levels followed by significant elevations of ALP in DDC-fed mice, compared to control mice (Fig. 8, A). Nevertheless, albumin levels, despite significantly slightly increased, fell into the "normal" range (Fig. 8, B-C). These results suggest that DDC feeding induces, already after 4 weeks, cholestasis and liver injury. However, at least until 16 weeks of DDC intoxication, experimental mice do not show liver failure, as suggested by albumin levels. For this reason, we decided to exclude albumin levels evaluation in all later experiments.

Gene expression analysis

At the molecular level, we evaluated the expression of some of the most common genes involved in the pathogenesis of fibrosis. In particular, we analyzed the expression of metalloproteinases (*Mmp2* and *Mmp9*) and the inhibitors of metalloproteinases (*Timp1* and *Timp2*), both involved in ECM remodelling, as well as the expression of the well-known pro-fibrogenic cytokine *Tgf*β[107,108]. Moreover, in literature it has been demonstrated that DDC mouse model develops, already at very early time points, a strong "Ductular Reaction" (DR)[109]. As previously discussed (see Introduction), this phenomenum involves the activation and proliferation of oval cells (i.e., bipotent progenitor cells resident in the adult liver), as well as their "differentiation" into the so-called reactive cholangiocytes[9]. For this reason, we analyzed also the expression of the most important cytokine (*Tweak*) and of its own receptor (*Fn14*), both involved in the activation and proliferation of oval cells[9].

As expected, all the above-mentioned genes significantly increased in experimental mice, compared to control ones (Fig. 8, D-E). In particular, their expression reached a peak after 4 weeks and then remained almost costant over time of DDC feeding. These results suggest that the most common and important fibrogenesis- and DR-related molecular players are strongly up-regulated in all the analyzed time points, thus substaining the progression of the CLD.

Histochemical stain

To further strengthen the obtained biometrical, serum and expression data, we directly analyzed the livers from an histological point of view. In particular, we performed PicroSirius Red (PSR) stain, which essentially puts in evidence the collagen deposition.

As expected from the previous data, PSR stain revealed a progressive accumulation of collagen. In particular, the so-called portal fibrosis (i.e., accumulation of ECM around the portal tract), observed after 4 weeks of DDC feeding, was subsequently followed by the appearance of the so-called portal-portal septa (i.e., fibrotic septa, linking portal tract to each other), which

became more and more numerous over time (Fig. 8, F). The histologic examination suggests that DDC feeding induces a progressive accumulation of ECM, thus disrupting the liver architecture.

Taking together, these findings suggest that DDC feeding of NSG mice, as already reported in the immunocompetent ones, induces cholestasis, liver injury and the development of a progressive fibrosis, without negatively affecting the hepatic functionality (at least during the whole observation period).

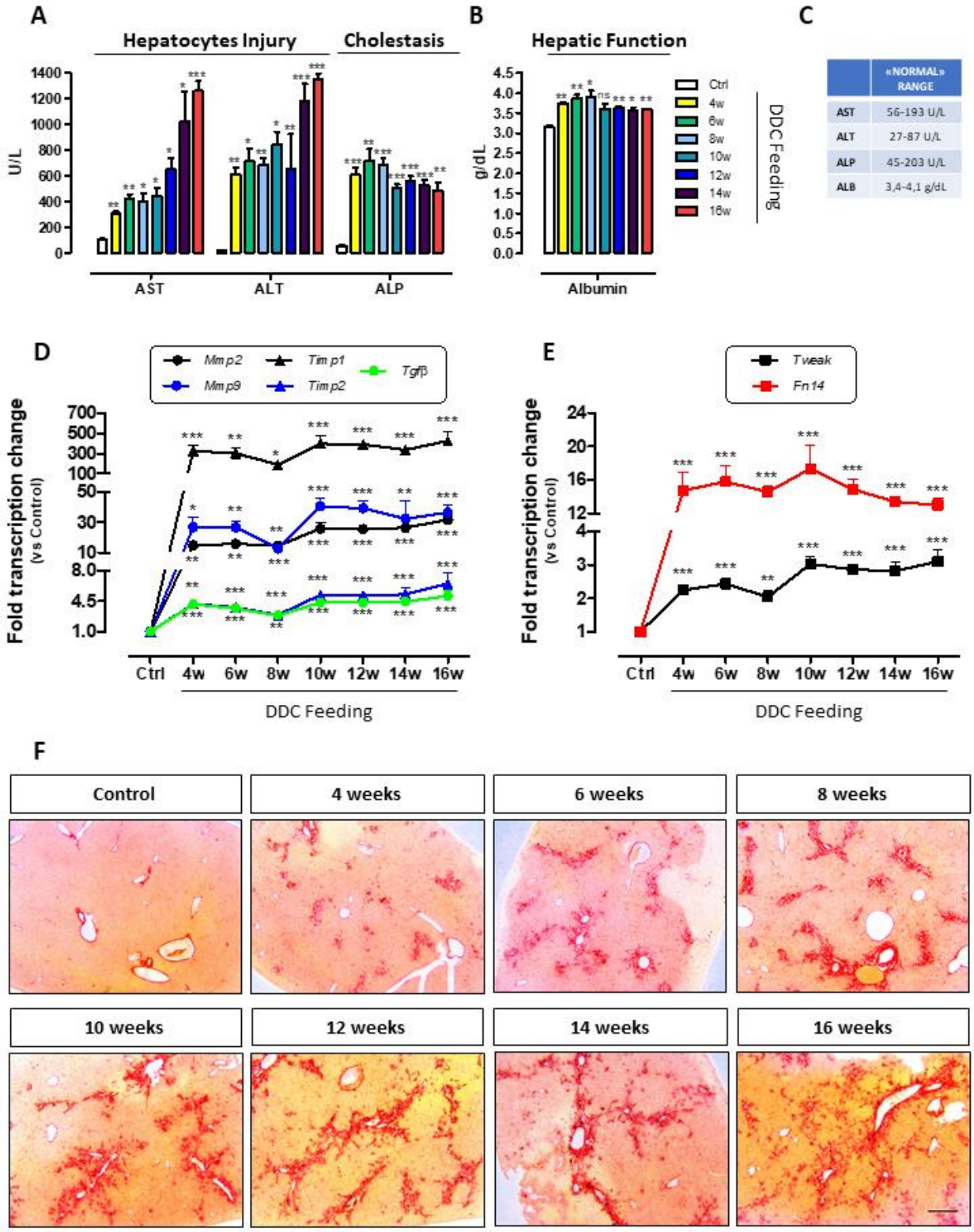

Figure 8. Longitudinal characterization of cholestatic and fibrotic phenotype following DDC intoxication. [A-B] AST and ALT, as well as ALP expressed as U/L and albumin expressed as g/dL were measured as biomarkers of hepatocytes injury, cholestasis and hepatic function, respectively, in control (Ctrl) mice and in DDC-fed mice sacrified at different time points. Data shown represent mean ± SEM. Unpaired t-test was performed: *p<0.05, **p<0.01, ***p<0.001. **[C]** Physiological range of these four parameters, reported by Charles River, in age-matched and sex-matched NSG mice. **[D-E]** Gene expression levels of fibrogenesis-related [D] and ductular reaction-related [E] genes in livers of mice fed with DDC-supplemented diet (at different time points) *versus* mice fed with standard diet (Ctrl). Data are expressed as mean ± SEM of relative quantification using the $2^{-\Delta\Delta Ct}$ method over cotrol (Ctrl) mice. Normalization was made using 18S as housekeeping gene. Unpaired t-test was performed: *p<0.05, **p<0.01, ***p<0.001. **[F]** Representative light microscopy micrographs of liver histology of both DDC-fed and control mice. Red stain represents collagen fibers considered to be a marker of liver fibrosis. Scale bar 0.05 cm.

HLSCs-derived EVs fail to recover Liver Fibrosis

A large array of works in animal models has shown that liver fibrosis is potentially reversible and, in specific circumstances, demonstrates a complete resolution with a restoration of near normal architecture[110]. Consistently, when the chronic stimulus is promptly removed, the liver may adapt itself to a new and permanent structure, which is probably compatible with a normal or near-normal function[111–113]. This spontaneous regression of liver damage, associated with the interruption of the toxic treatment, reported in mice and rats could hamper the use of these models to test the value of therapeutics and innovative tratments[114–116]. For this reason, before starting with the administration of HLSCs-derived EVs in fibrotic mice, we have firstly questioned about the possibility of maintaining DDC diet or returning to standard diet during the treatment with EVs. Therefore, we assessed the potential reversibility of the cholestatic and fibrotic phenotype observed in 8 weeks DDC-fed mice, by allowing an additional group of animals to return to the standard diet for 2 other weeks (Recovery mice). Then, we compared the recovery mice to both 8 weeks and 10 weeks DDC-fed mice, as well as to the standard diet-fed control mice. In this way, we were able to understand if the removal of DDC diet is simply able to slowdown or block the progression of fibrosis or to even induce its (partial or full) regression.

Regarding serum biochemical analysis, AST, ALT and ALP levels significantly and massively decreased in recovery mice, compared to 10 weeks DDC-fed mice and even to the 8 weeks ones. Moreover, their levels were perfectly comparable to the levels of control mice, thus suggesting that they fell again into their “physiological” range (Fig. 9, A). Similarly, at the molecular level, all the analyzed genes were significantly down-regulated in recovery mice, compared to both 8 weeks and 10 weeks DDC-fed mice (Fig. 9, B). However, with the exception of *Fn14* and *Mmp9*, all the other genes still showed a significant but slight increase in recovery mice, compared to control ones (Fig. 9, B). Of interest, the most important and convincing evidence, regarding the reversibility of the fibrotic phenotype, came from PSR stain of liver slices. Liver fibrosis in recovery mice was less pronounced respect to 10 weeks DDC-fed mice and even respect to 8 weeks DDC-fed mice, suggesting that there was not a slowdown or block of liver fibrosis progression but a substantial regression (Fig. 9, C).

Taking together, these results suggest that the removal of toxic stimulus (i.e., DDC diet) is sufficient to induce a strong, altough partial, recovery of the cholestatic and fibrotic phenotype. This means that could be difficult, or even impossible, to discriminate between a spontanuous regression and the EVs-mediated regression. Based on this observation, we decided to maintain the DDC diet during the treatment with the HLSCs-derived EVs.

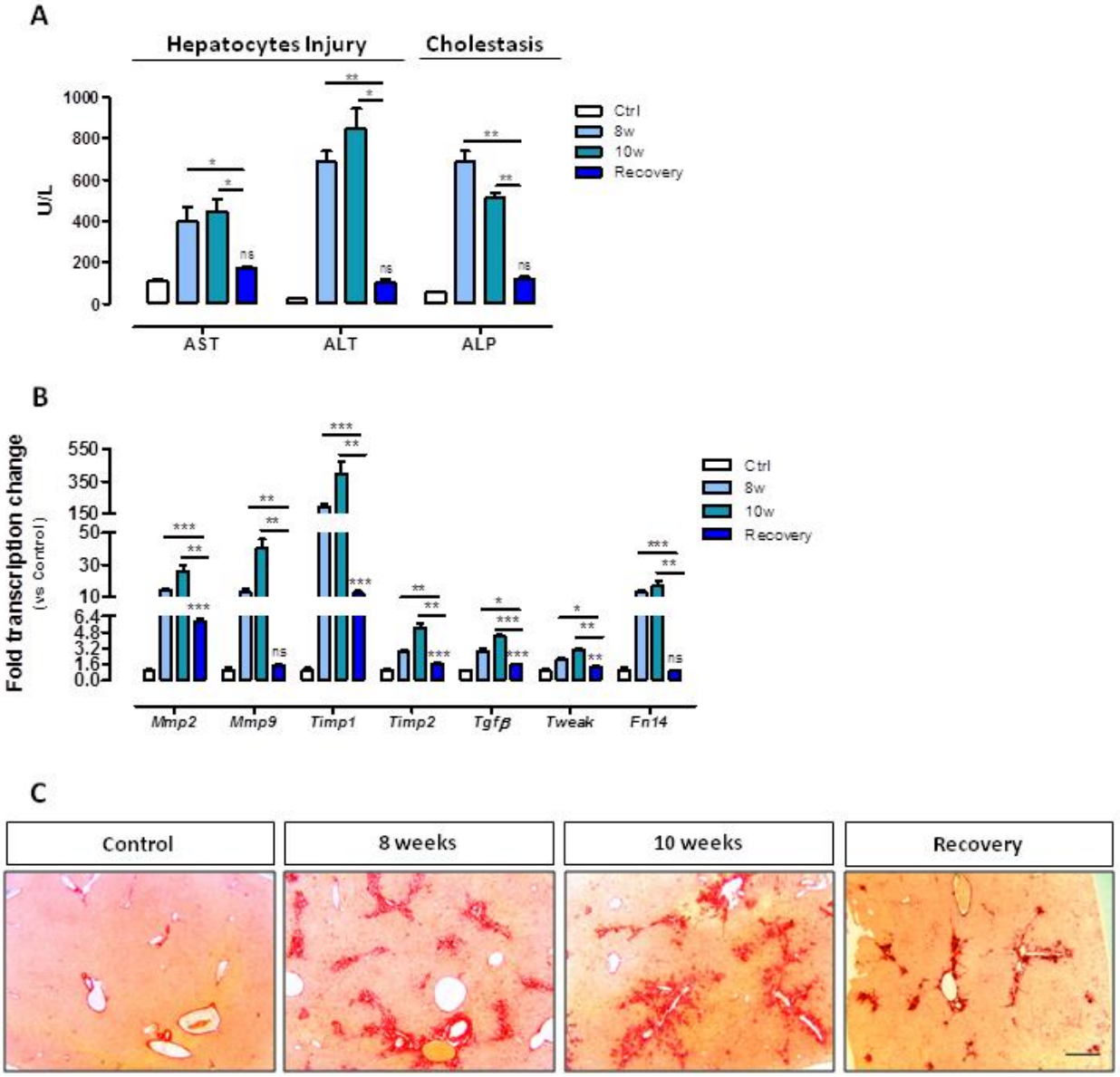

Figure 8. Evaluation of cholestatic and fibrotic phenotype reversibility after DDC removal. [A] AST and ALT, as well as ALP expressed as U/L were measured as biomarkers of hepatocytes injury and cholestasis, respectively, in control (Ctrl) mice, in DDC-fed mice sacrified at 8 and 10 weeks (8w and 10w) and in recovery mice. Data shown represent mean ± SEM. Unpaired t-test was performed: *p<0.05, **p<0.01, ***p<0.001. **[B]** Gene expression levels of fibrogenesis-related and ductular reaction-related genes in livers of control (Ctrl) mice, DDC-fed mice sacrified at 8 and 10 weeks (8w and 10w) and recovery mice. Data are expressed as mean ± SEM of relative quantification using the $2^{-\Delta\Delta Ct}$ method over control (Ctrl) mice. Normalization was made using 18S as housekeeping gene. Unpaired t-test was performed: *p<0.05, **p<0.01, ***p<0.001. **[C]** Representative light microscopy micrographs of liver histology of control, DDC-fed and recovery mice. Red stain represents collagen fibers considered to be a marker of liver fibrosis. Scale bar 0.05 cm.

After having assessed the natural history of DDC-induced CLD and its reversibility, we started evaluating the therapeutic effect of HLSCs-derived EVs, by injecting them into DDC-induced fibrotic mice. Of interest, it should be noted that there are a lot of variables, which should be taken into account. For example, the timing at which start and end the treatment, the dose of EVs to be administrated, as well as the weekly frequency of injections. Therefore, based on all these variables, we designed three different therapeutic regimens (Fig. 10). In this sense, however, important hints came from the literature[117–119].

Concerning the first one, we performed a single injection a week of $1x10^8$ HLSCs-derived EVs, by starting and ending their administration after 4 and 8 weeks of DDC intoxication, respectively (Fig. 10, A). Overall, these mice received in total four injections, distributed in 4 weeks. Concerning the second regimen, we decided to maintain the previous setting and to change only the dose. In particular, we injected $2,5x10^9$ HLSCs-derived EVs (Fig. 10, B). Lastly, concerning the third regimen, we decided to anticipate the start/end point of the treatment at 2 and 4 weeks of DDC feeding, respectively, and to performe two injections a week of $2,5x10^9$ HLSCs-derived EVs (Fig. 10, C). Overall, also these mice received in total four injections, but distributed in only 2 weeks. Similarly, in all the above-mentioned experiments, control mice were treated with the vehicle (PBS), by following the respective regimen. After 3 days from the last injection, experimental and control mice were sacrified and their sera and livers were analyzed by following our standardized work-up, with the exception of albumin levels evaluation, as stated before (Fig. 7, B).
The description of the three regimens coincides with the chronological order of the experiments, thus meaning that they were carried out and suitably modified one after the other.

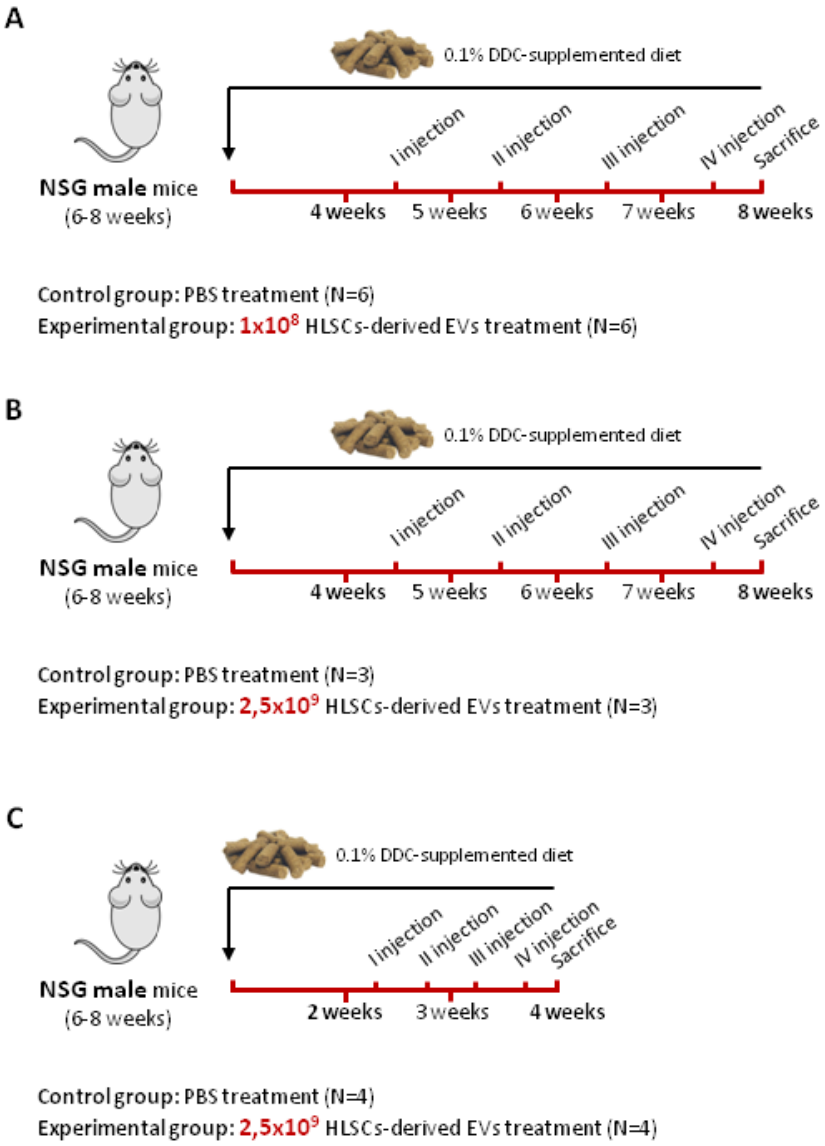

Figure 10. Therapeutic regimens. **[A]** In the first experiment, $1x10^8$ EVs were injected once weekly for 4 weeks, starting after 4 weeks of DDC feeding. **[B]** In the second experiment, $2,5x10^9$ EVs were injected once weekly for 4 weeks, starting after 4 weeks of DDC feeding. **[C]** In the third and last experiment, $2,5x10^9$ EVs were injected twice weekly for 2 weeks, starting after 2 weeks of DDC feeding. In all the experiments, DDC diet was administered also during the timing of EVs injections.

In all the experiments, EVs-treated mice did not show any differences in terms of liver and spleen weight (Fig. 11, A-B-C), serum biochemistry (Fig. 11, D-E-F), fibrogenesis- and DR-related gene expression levels (Fig. 12), as well as in terms of collagen deposition (Fig. 13).

Taking together, these findings suggest that HLSCs-derived EVs may not exhibit therapeutic effects in our DDC-induced fibrotic mice.

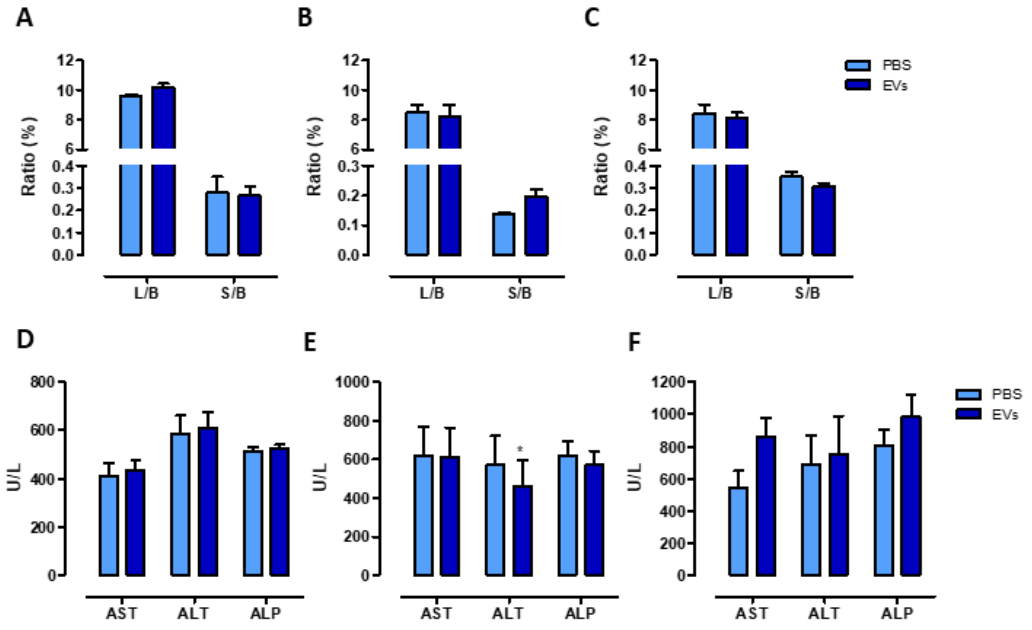

Figure 11. Biometric "clinical" data and serum tests after HLSCs-derived EVs treatment. [A-B-C] Body, Liver and Spleen weight of PBS- and EVs-treated mice were recorded upon harvesting. Liver/Body (L/B) weight ratio and Spleen/Body (S/B) weight ratio, expressed as percentage (%), are indexes of hepatomegaly and splenomegaly, respectively. A, B, C represent the first, second and third experiment, respectively. Data shown represent mean ± SEM. Statistically significant differences were evaluated using unpaired t-tests. **[D-E-F]** AST and ALT, as well as ALP expressed as U/L were measured as biomarkers of hepatocytes injury and cholestasis and hepatic function, respectively, in PBS- and EVs-treated mice. D, E, F represent the first, second and third experiment, respectively. Data shown represent mean ± SEM. Unpaired t-test was performed: *p<0.05.

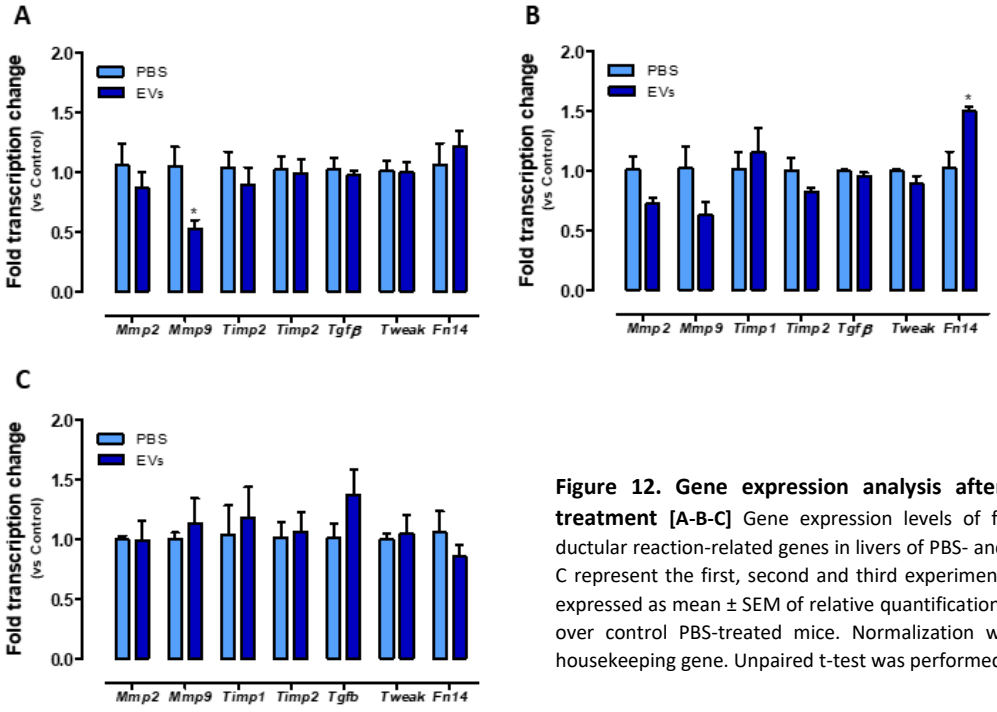

Figure 12. Gene expression analysis after HLSCs-derived EVs treatment [A-B-C] Gene expression levels of fibrogenesis-related and ductular reaction-related genes in livers of PBS- and EVs-treated mice. A, B, C represent the first, second and third experiment, respectively. Data are expressed as mean ± SEM of relative quantification using the $2^{-\Delta\Delta Ct}$ method over control PBS-treated mice. Normalization was made using 18S as housekeeping gene. Unpaired t-test was performed: *p<0.05.

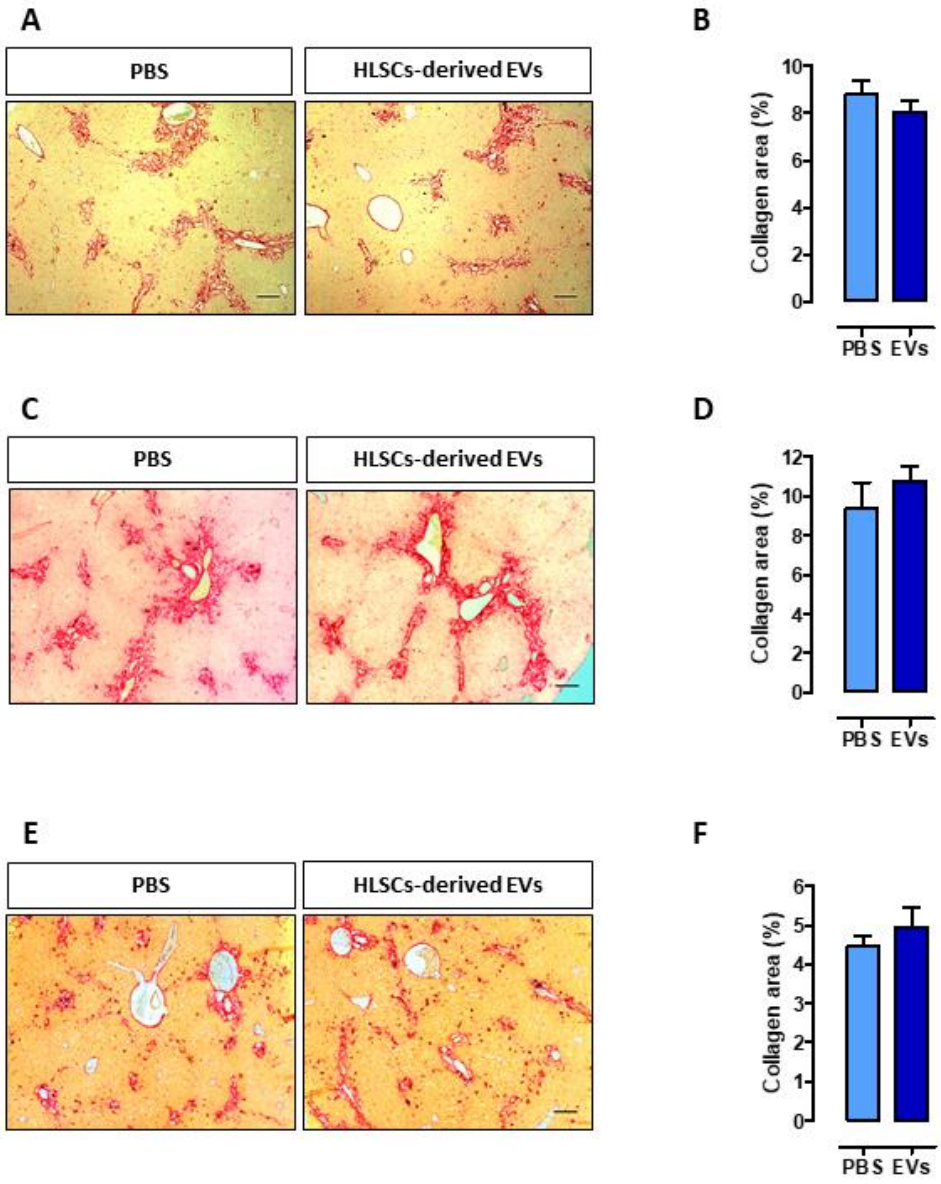

Figure 13. Histologic evaluation after HLSCs-derived EVs treatment. [A-C-E] Representative light microscopy micrographs of liver histology of PBS- and EVs-treated mice. A, C, E represent the first, second and third experiment, respectively. Red stain represents collagen fibers considered to be a marker of liver fibrosis. Scale bar 0.2 mm. **[B-D-F]** Quantification of red area (corresponding to collagen) normalized to the total area and, therefore, expressed as percentage (%). >5 fields for each mouse. B, D, F represent the first, second and third experiment, respectively. Data shown represent mean ± SEM. Statistically significant differences were evaluated using unpaired t-tests.

HLSCs-derived EVs do not reach Cholestasis-induced Fibrotic Liver

Bruno S. *et al.* recently demonstrated that HLSCs-derived EVs exhibit anti-fibrotic effects in a NASH murine model[120]. Therefore, our data may seem controversial.

Why were not we able to observe the same anti-fibrotic effects?

Despite the underlying mechanisms are still not fully understood, in literature it has been widely accepted the concept that EVs are able to preferentially reach a damaged site, where they can explicate their regenerative effects[118,120,121]. Consistently, the authors of the above-mentioned work demonstrated that EVs injected through a systemic route, namely the tail vein,

were mostly localized into the damaged liver, compared to the other analyzed organs[120]. Therefore, taking into account the hints from the literature, we decided to inject the HLSCs-derived EVs directly into the tail vein (see Material and Methods). However, even though in literature is emerging and strengthening over time this general consensus about the homing of EVs to the damaged site, we decided to assess the bio-distribution of labeled-EVs specifically in our DDC-induced fibrosis mouse model, compared to the standard diet-fed control mice. Consistently, the experimental workflow consisted in [1] injecting fluorescent labeled-EVs into the tail vein of 2 weeks (i.e., the start point of the third regimes) DDC diet- and standard diet-fed mice and in [2] analyzing several organs with optical imaging (In Vivo Imaging Systems, IVIS).

By looking at the healthy control mice-derived organs, we observed a prominent accumulation of fluorescent labeled-EVs in the liver, whereas the signal in the other organs was nearly absent (Fig. 14, A). This could be due to the physiological clearance activity and high permeability of the liver. Surprisingly, by comparing the livers of DDC-induced fibrotic mice and healthy control mice, we observed a strong signal in normal liver, whereas no signal in damaged/fibrotic liver (Fig. 14, B-C).

Taking together, these results surprisingly suggest that in DDC-induced fibrotic mice HLSCs-derived EVs are not able anymore to accumulate into the liver. Therefore, thanks to the bio-distribution data, we can clearly and surely answer to our previous question. We were not able to appreciate any therapeutic effects in our DDC murine model because of the inability of HLSCs-derived EVs to reach the damaged liver and, consequently, to exert their potential anti-fibrotic and regenerative effects.

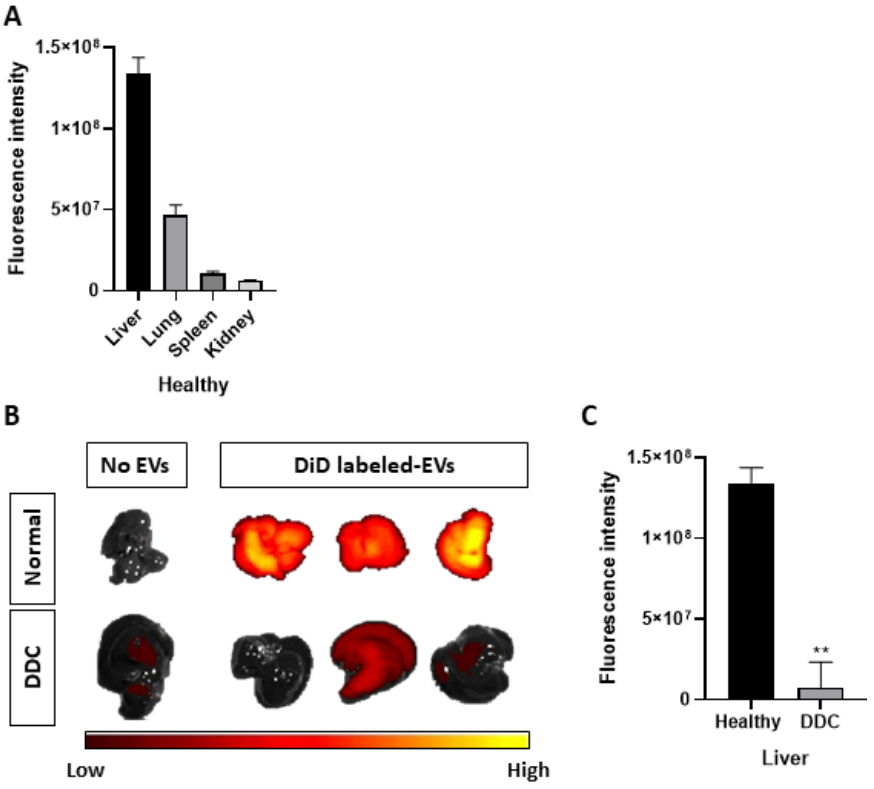

Figure 14. IVIS biodistribution of fluorescent labeled-EVs. [A] Quantification of fluorescence intensity in dissected organs of healthy mice, measured as average radiance ± SEM at 3h post-EVs administration (N=3). **[B]** Representative images obtained by optical imaging of livers of healthy and DDC intoxicated mice, collected 3h after EVs or vehicle administration. [C] Quantification of fluorescence intensity in livers of healthy and DDC-intoxicated mice injected with fluorescent EVs (N=3). Statistically significant differences were evaluated using unpaired t-tests: **p<0.01.

Basic Approach

FLVCR1a positively regulates LSECs fenestration: Implications for Liver Homeostasis and Liver Fibrosis

FLVCR1a is particularly expressed in murine LSECs compared to the other tissue-specific microvascular ECs

In our body, to encounter each organ specific physiological function, microvascular endothelial cells undergo a process of specialization and differentiation (i.e., vascular organotypicity)[43]. Interestingly, the well-known morphological classification of capillaries it has been recently found to be associated to a unique gene expression profile[122]. In fact, Nolan D.J. *et al.* few years ago highlighted the molecular heterogeneity of microvascular ECs, by performing microarray analysis on ECs derived from different murine tissues, such as liver, lung and so on[122].

As previously discussed (see Introduction), during the last years it has been shown that FLVCR1a plays a key role in endothelial cells during embryo development. Nevertheless, its role in adult quiescient ECs has never been investigated so far. Therefore, by considering the recently highlighted angiodiversity at the molecular level, we interrogated these public microarray gene expression data[122] for *Flvrcr1a* expression levels. Two Flvcr1 probes have been found (i.e., #10361075 and #10361065). Interestingly, *Flvcr1a* is particularly expressed in murine LSECs compared to the other tissue-specific microvascular ECs, as well as it is likely to be nearly absent in testicle- and heart-derived ECs (Fig. 15).

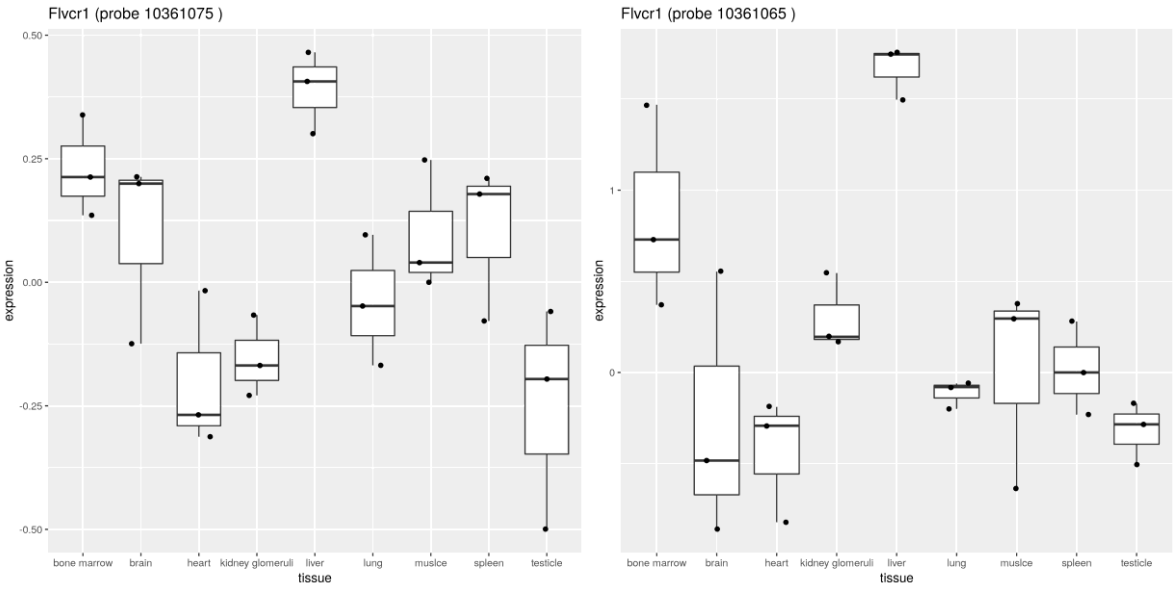

Figure 15. Gene expression levels of *Flvcr1* in tissue-specific murine ECs. *Flvcr1* is represented by two probes on the microarray. The expression of the two probes in the tissues is represented in the following plots. Expression levels above 0 can be considered indicating detection. This means that with expression "0" we can speculate that the gene is nearly absent.

Gain- and Loss-of-FLVCR1a expression do not affect total Heme and ROS levels as well as cell viability in an *in vitro* model of human LSECs

To unveil the biological role of the heme exporter FLVCR1a in LSECs, we performed gain- and loss-of-function *in vitro* assays. In particular, we used an human cell line, namely Sk-Hep1, which resembles many features of primary LSECs, such as the presence of fenestrae and the lack of CD31 expression[123]. Firstly, we transduced Sk-Hep1 cells in order to generate both FLVCR1a-overexpressing and FLVCR1a-silenced cell lines, as well as their respective controls (Fig. 16, A). The expression of FLVCR1b isoform (i.e., the mitochondrial heme exporter) was not affected, upon FLVCR1a levels modulation (Fig. 16, A).
As previously discussed (see Introduction), heme is an essential co-factor in multiple biological processes[93]. Nevetherless, excess free-heme is highly toxic due to its ability to promote ROS production, thus ultimately leading to apoptosis. Thus, heme metabolism needs to be finely regulated. Consistently, intracellular heme amount is controlled at multiple levels. For example, it has been shown that FLVCR1a exports, from the cytosol toward the extracellular space, the excessive heme[93]. Therefore, we measured [1] heme and [2] ROS levels, as well as [3] cell viability in this specific cellular model, upon FLVCR1a modulation.

Both FLVCR1a-overexpressing and FLVCR1a-silenced cell lines did not exhibit differences in terms of both heme and ROS levels, compared to their respective controls (Fig. 16, B). Therefore, it is not so surprising that FLVCR1a modulation did not have an impact on cell viability (Fig. 16, C-D-E).

Taking together, these findings suggest that this specific sinusoidal endothelial cell line is able to compensate some how the up- or down-regulation of FLVCR1a, thus maintaining into normal range both heme and ROS levels and, in turn, thus preserving cell viability. Fiorito V. *et al.* recently showed that, to maintain heme levels into a physilogical range, heme exporter and heme synthesis are tighly linked and that they regulate one to each other (under revision). In particular, a high heme exporter activity leads to an high heme synthesis and, on the contrary, a low heme exporter activity leads to a low heme synthesis (under revision). For this reason, as later discussed, we hypothesized that heme levels do not change because of heme synthesis compensation following the FLVCR1a modulation in Sk-Hep1 cells.

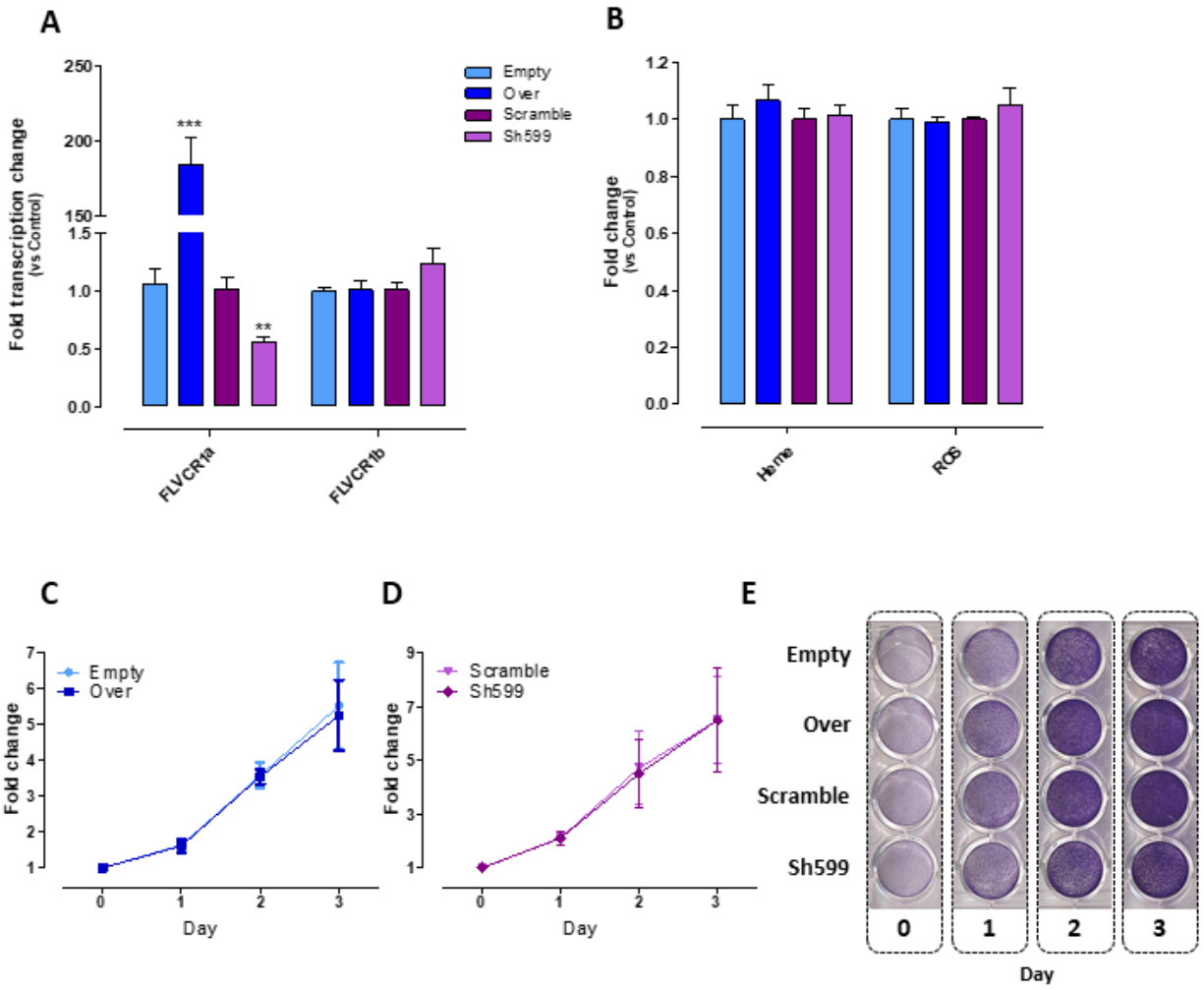

Figure 16. "General" characterization of Sk-Hep1 cells upon FLVCR1a levels modulation. [A] Gene expression levels of *FLVCR1a* and *FLVCR1b*. Normalization was made using 18S as housekeeping gene. Data are expressed as mean ± SEM of relative quantification using the $2^{-\Delta\Delta Ct}$ method over their respective controls (N=8). Unpaired t-test was performed: *p<0.05, **p<0.01, ***p<0.001. **[B-C]** Heme [B] and ROS [C] levels upon FLVCR1a overexpression and silencing are expressed as a fold increase over their respective controls (N=3, n=2). Unpaired t-test was performed. **[D-E]** Cell viability was assessed through crystal violet assay. Values are expressed as fold increase at 1, 2, 3 days over day 0 (namely 24h after plating). Data are expressed as mean ± SEM (N=4, n=4 Empty and Over, N=3, n=4 Scramble and Sh599). Unpaired t-test was performed. **[F]** Representative images of cells stained with crystal violet at the analyzed time points. Over: FLVCR1a-overexpressing cells; Empty: respective control; Sh599: FLVCR1a-silenced cells; Scramble: respective

FLVCR1a levels positively correlate with Membrane Fluidity

As previously discussed (see Introduction), the presence of both "open" (i.e., without diaphragm) fenestrae and a disorganized basement membrane distinguishes LSECs from all the other endothelial cells, thus making them unique in our body. Due to the enrichment of FLVCR1a expression specifically in LSECs compared to other tissue-specific endothelial cells, we started questioning about the possible involvement of FLVCR1a in the maintenance of fenestration.

Despite the first observation of LSECs fenestration dates to 1970s[46], the molecular and structural mechanisms underlying the formation, maintenance and dynamic regulation of LSECs fenestrae are still elusive. This is because one of the major challenges in studying LSECs biology is related to technical and methodological limitations. In particular, due to the small diameter

of these pores (namely 100-200 nm), nowadays, the gold standard method to detect and measure LSECs fenestrae is Scanning Electron Microscopy analysis (SEM), both *in vitro* and *in vivo*. However, SEM is a laborious technique that requires uncommon equipment, as well as specific skills related to sample processing, images acquisition and, most importantly, images interpretation. For this reason, to overcome this technical issue, we firstly started finding an alternative and indirect approach to assess LSECs fenestration *in vitro*. In this sense, important cues came from the literature[124,125]. It has been proposed the hypothesis that fenestrae originate from a process of membrane invagination and, consequently, from its fusion with basolateral membrane. Consistently, the physical-chemical properties of plasma membrane are extremely important. In particular, a reduced membrane tension, due to cholesterol depletion, leads to membrane invaginations. On the contrary, an increased membrane tension, due to cholesterol accumulation, hampers these invaginations[124,125]. Therefore, membrane fluidity could be a reliable indirect parameter of cells fenestration capability.

To assess whether membrane fluidity could effectively be indicative of the presence of fenestrae, we treated Sk-Hep1 cells with Cytochalasin D and Antimycin A, which essentially are well-known positive and negative regulators of fenestrae, respectively[126]. As hypothesized, Cytochalasin D treatment increased membrane fluidity, whereas Antimycin A treatment descreased it (Fig. 17, A). Subsequently, we measured membrane fluidity in both FLVCR1a-overexpressing and FLVCR1a-silenced cell lines. The first one exhibited a more fluid membrane, wheares the second one exhibited a more rigid membrane, compared to their respective controls (Fig. 17, B).

Taking together, these results suggest that [1] membrane fluidity could be a reliable indirect parameter of Sk-Hep1 fenestration and that [2] FLVCR1a positively regulates membrane fluidity, thus allowing us to speculate that FLVCR1a can positively regulate fenestrae formation and/or maintenance. These results are perfectly in concordance with the previous microarray data showing enriched expression of FLVCR1a in fenestrated LSECs, compared to the other tissue-specific endothelial cells. Overall, FLVCR1a could be regarded as an important player in the formation and/or maintenance of LSECs fenestrae and, consequently, of liver homeostasis.

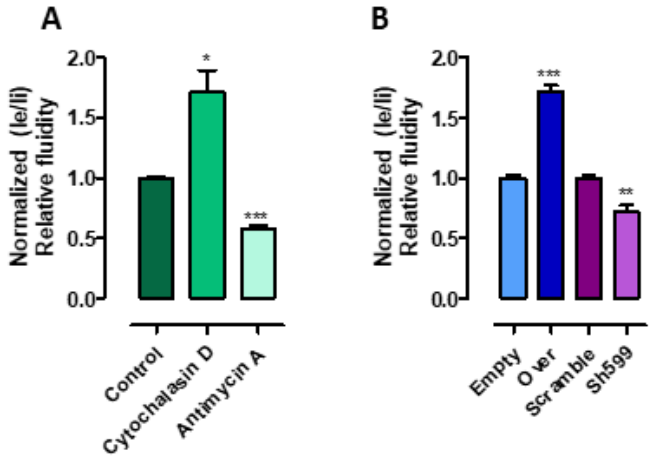

Figure 17. Membrane fluidity assay. [A] Sk-Hep1 cells were treated for 1h with 2 µM Cytochalasin D and 1 µg/ml Antimycin A, positive and negative control of LSECs fenestration, respectively. Membrane fluidity is expressed as fold increase of normalized Ie/Ii (corresponding to eximer and monomer fluorescence, respectively) fluorescence over not-treated control cells. Data are expressed as mean ± SEM (N=3, n=3). Unpaired t-test was performed: *p<0.05, **p<0.01, ***p<0.001. **[B]** Membrane fluidity is expressed as fold increase of normalized Ie/Ii (corresponding to eximer and monomer fluorescence, respectively) fluorescence over their respective controls. Data are expressed as mean ± SEM (N=3, n=3). Unpaired t-test was performed: *p<0.05, **p<0.01, ***p<0.001. Over: FLVCR1a-overexpressing cells; Empty: respective control; Sh599: FLVCR1a-silenced cells; Scramble: respective control.

FLVCR1a modulation has an impact on Cholesterol Synthesis and on Membrane Cholesterol content

After having highligthed a positive correlation between FLVCR1a levels and membrane fluidity, we deeper investigated the underlying mechanisms.
As mentioned in the previous paragraph, membrane cholesterol content is a critical determinant in membrane tension and, consequently, in fenestrae formation. For this reason, we measured the levels of cholesterol in both FLVCR1a-overexpressing and FLVCR1a-silenced cells-derived membranes. We observed that FLVCR1a levels inversely correlate with membrane cholesterol content. In particular, FLVCR1a-overexpressing cells and FLVCR1a-silenced cells exhibited low and high levels of cholesterol in membrane, respectively, compared to their controls (Fig. 18, A). These results suggest that FLVCR1a may regulate the membrane fluidity by affecting its cholesterol content.

How can FLVCR1a have an impact on membrane cholesterol content?

Fiorito V. *et al.* recently showed that, by "simply" modulating FLVCR1a levels, a general metabolic rewiring is obtained (under revision). Taking into account this finding, to answer to the previous question, we decided to directly assess the cholesterol synthesis rate. Consistently, we incubated cells with a radiolabeled cholesterol precursor and, after 24h, we quantified the produced radiolabeled cholesterol. FLVCR1a-overexpressing cells and FLVCR1a-silenced cells exhibited low and high cholesterol synthesis rate, respectively, compared to their controls (Fig. 18, B). These results suggest that a different cholesterol synthesis rate can be the cause of the different cholesterol content in membrane.

Taking together, these results strongly suggest that FLVCR1a can influence the membrane physical-chemical properties, namely its cholesterol content, by negatively regulating the synthesis of cholesterol.

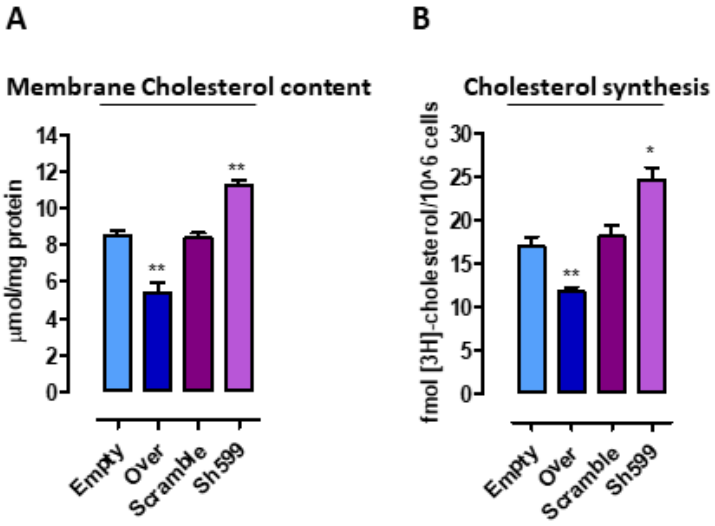

Figure 18. Impact on cholesterol metabolism following FLVCR1a levels modulation. **[A]** Cholesterol content in plasma membrane is expressed as µmol/mg protein. Data are expressed as mean ± SEM (N=3). Unpaired t-test was performed: *p<0.05, **p<0.01, ***p<0.001. **[B]** Rate *de novo* cholesterol synthesis is expressed as fmol of radiolabeled cholesterol over $1x10^6$ cells. Data are expressed as mean ± SEM (N=3, n=3). Unpaired t-test was performed: *p<0.05, **p<0.01, ***p<0.001. Over: FLVCR1a-overexpressing cells; Empty: respective control; Sh599: FLVCR1a-silenced cells; Scramble: respective control.

Membrane Fluidity strictly depends on the correct balance between both Heme and Cholesterol Synthesis

The TriCarboxylic Acid cycle (TCA cycle), also known as Krebs cycle, in the mitochondria is the central process in energy metabolism, as well as in the biosynthetic pathway[127]. In fact, intermediates leave the cycle to be used as precursor for a variety of macromolecules. This process is termed "cataplerosis". However, if TCA cycle anions are removed from the cycle, they must be replaced to permit its continued function. This process is termed "anaplerosis". Therefore, anaplerosis and cataplerosis work together to ensure the appropriate balance of carbon flow into and out of the TCA cycle, thus avoiding the accumulation or the depletion of TCA intermediates. However, also the different cataplerotic pathways could be balanced to each other.
Heme synthesis and cholesterol synthesis are both considered cataplerotic pathways. In fact, succinyl-CoA and citrate are TCA intermediates that leave the cycle to be converted (through several enzymatic reactions) to heme and cholesterol, respectively. As previously discussed, both FLVCR1a-overexpressing and FLVCR1a-silenced cell lines did not exhibit differences in terms of heme levels, compared to their respective controls (Fig. 16, B). Since our group recently showed that, to maintain heme levels into a physilogical range, heme export and heme synthesis are tighly linked, we hypothesized that heme levels do not change because of heme synthesis compensation following the FLVCR1a modulation in Sk-Hep1 cells (under revision). The consequence could be a dysregulation of the other cataplerotic and anaplerotic patwhays. In fact, following FLVCR1a modulation, we observed an effect on cholesterol synthesis rate. (Fig. 18, B). Of interest, in FLVCR1a-overexpressing cells, for example, heme could be synthesized at higher rate, thus slowing down the other cataplerotic pathways, such as the conversion of citrate into cholesterol. This means that heme synthesis and cholesterol synthesis could be tighly linked. To validate this hypothesis, we "shut down" the (potential) high succinyl-CoA utilization in FLVCR1a-overexpressing cells, with the idea to rescue the cholesterol synthesis, the cholesterol in membrane and, consequently, the membrane fluidity.

How can we "shut down" the succinyl-CoA utilization?

The process of heme synthesis consists of eight enzymatic reactions and initiates in mitochondria with the condensation of glycine and succinyl-CoA to form δ-AminoLevulinic Acid (ALA). This first reaction is catalyzed by Amino Levulinic Acid Synthase (ALAS), the rate-limiting enzyme in heme biosynthetic pathway. ALAS1 isoform, differently from ALAS2 isoform, is ubiquitously expressed and, most importantly, is controlled at different levels (e.g., transcription, translation and localization) by heme itself through a negative feedback[128,129]. Therefore, high heme levels shut down the ALAS1-mediated utilization of succinyl-CoA, thereby preventing further heme production.
In literature, it has been widely demonstrated that ALA-treated cells exhibit the accumulation of the subsequent intermediates of heme biosynthetic pathway, among them ProtoPorphyrin IX (PPIX), and the accumulation of heme, the final product[128]. This means that, by treating cells directly with ALA, the rate-limiting step is bypassed and ALA can be "freely" converted, through the other enzymatic reactions, to PPIX and heme. However, paradoxically, this initial transient high PPIX and heme levels could be later followed by a negative regulation of ALAS1, thus preventing the endogenous *de novo* synthesis of heme by starting from endogenous succinyl-

CoA of the TCA cycle. Consistently, to support this hypothetical paradox, we treated Sk-Hep1 cells with ALA and then we [1] measured Heme, PPIX and ROS levels, as well as we [2] assessed the expression levels of *ALAS1*. As expected, ALA treatment induced a significant increase of both heme and PPIX levels, whitout however triggering ROS production (Fig. 19, A). Of interest, ALA treatment induced a strong down-regulation of *ALAS1* expression, suggesting that there could be a decreased activity of ALAS1 (Fig. 19, B). Overall, based on these results, we decided to "shut down" the (potential) high succinyl-CoA utilization in FLVCR1a-overexpressing cells, by treating them with ALA. Firstly, we ascertained that the treatment with ALA did not affect the viability of FLVCR1a-overexpressing cells (Fig. 19, C). Subsequently, to validate the hypothesized link between heme and cholesterol synthesis, we [1] measured the cholesterol synthesis rate in ALA-treated FLVCR1a-overexpressing cells and then we [2] compared it to both vehicle-treated FLVCR1a-overexpressing cells and empty control cells rate. The treatment with ALA, namely the inhibition of ALAS1-mediated succinyl-CoA utilization, was sufficient to rescue the cholesterol synthesis. In particular, ALA-treated FLVCR1a-overexpressing cells exhibited a higher cholesterol synthesis rate, compared to vehicle-treated ones, thus reaching the same rate observed in the empty control cells (Fig. 19, D). As a consequence, by rescueing the cholesterol synthesis rate, we were able to rescue also the membrane cholesterol content, as well as the membrane fluidity (Fig. 19, E-F).

Taking together, these results suggest that, as previously hypothesized, [1] FLVCR1a-overexpressing cells exhibit a higher ALAS1-mediated succinyl-CoA consumption and that [2] cholesterol synthesis rate strictly depends on ALAS1 activity and succinyl-CoA consumption.

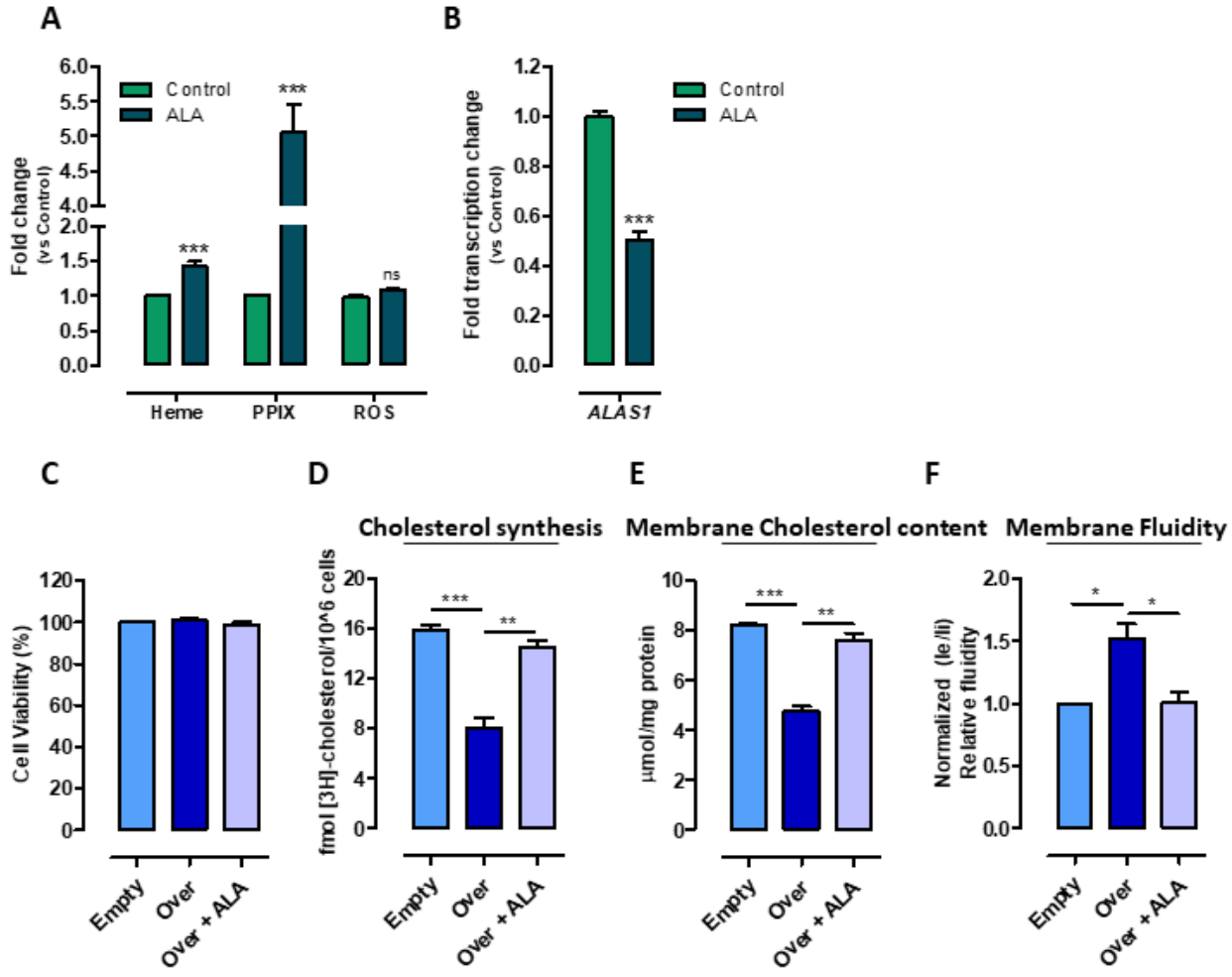

Figure 19. Cholesterol metabolism strictly depends on ALAS1-mediated succinyl-CoA consumption. [A] Heme, PPIX and ROS levels upon 24h of 5mM ALA treatment are expressed as a fold increase over the vehicle-treated control. Data are expressed as mean ± SEM (N=3, n=2). Unpaired t-test was performed: *p<0.05, **p<0.01, ***p<0.001. **[B]** Gene expression levels of *ALAS1* upon 24h of 5 mM ALA treatment. Normalization was made using 18S as housekeeping gene. Data are expressed as mean ± SEM of relative quantification using the $2^{-\Delta\Delta Ct}$ method over vehicle-treated control cells (N=3). Unpaired t-test was performed: *p<0.05, **p<0.01, ***p<0.001. **[C]** Cell viability was assessed thourgh crystal violet assay. Values are expressed as percentage (%) compared to control cells (Empty). Data are expressed as mean ± SEM (N=3, n=4). Unpaired t-test was performed: *p<0.05, **p<0.01, ***p<0.001. **[D]** Rate *de novo* cholesterol synthesis is expressed as fmol of radiolabeled cholesterol over $1x10^6$ cells. Data are expressed as mean ± SEM (N=3, n=3). Unpaired t-test was performed: *p<0.05, **p<0.01, ***p<0.001. **[E]** Cholesterol content in plasma membrane is expressed as µmol/mg protein. Data are expressed as mean ± SEM (N=3). Unpaired t-test was performed: *p<0.05, **p<0.01, ***p<0.001. **[F]** Membrane fluidity is expressed as fold increase of normalized Ie/Ii (corresponding to eximer and monomer fluorescence, respectively) fluorescence over their respective controls. Data are expressed as mean ± SEM (N=3, n=3). Unpaired t-test was performed: *p<0.05, **p<0.01, ***p<0.001. Empty: control; Over: FLVCR1a-overexpressing cells; Over + ALA: FLVCR1a-overexpressing cells treated for 24h with 5 mM ALA (rescue condition).

On the other hand, FLVCR1a-silenced cells could exhibit a low heme synthesis rate, thus strongly sustaining the efflux of citrate from mitochondria to cytoplasm and its conversion into cholesterol. To validate this hypothesis, we blocked the (potential) high citrate efflux in FLVCR1a-silenced cells, with the idea to rescue the cholesterol synthesis, the cholesterol in membrane and, ultimately, the membrane fluidity.

Firstly, we ascertained that the treatment with the inhibitor of the citrate carrier (iCIC) did not affect the viability of FLVCR1a-silenced cells (Fig. 20, A). Subsequently, to validate the hypothesized link between citrate efflux and cholesterol synthesis, we [1] measured the

cholesterol synthesis rate in iCIC-treated FLVCR1a-silenced cells and then we [2] compared it to both vehicle-treated FLVCR1a-silenced cells and scramble control cells rate. The treatment with iCIC, namely the inhibition of citrate efflux, was sufficient to rescue the cholesterol synthesis. In particular, iCIC-treated FLVCR1a-silenced cells exhibited a lower cholesterol synthesis rate, compared to vehicle-treated ones, thus reaching the same rate observed in the scramble control cells (Fig. 20, B). As a consequence, by rescueing the cholesterol synthesis rate, we were able to rescue also the membrane cholesterol content, as well as the membrane fluidity (Fig. 20, C-D).

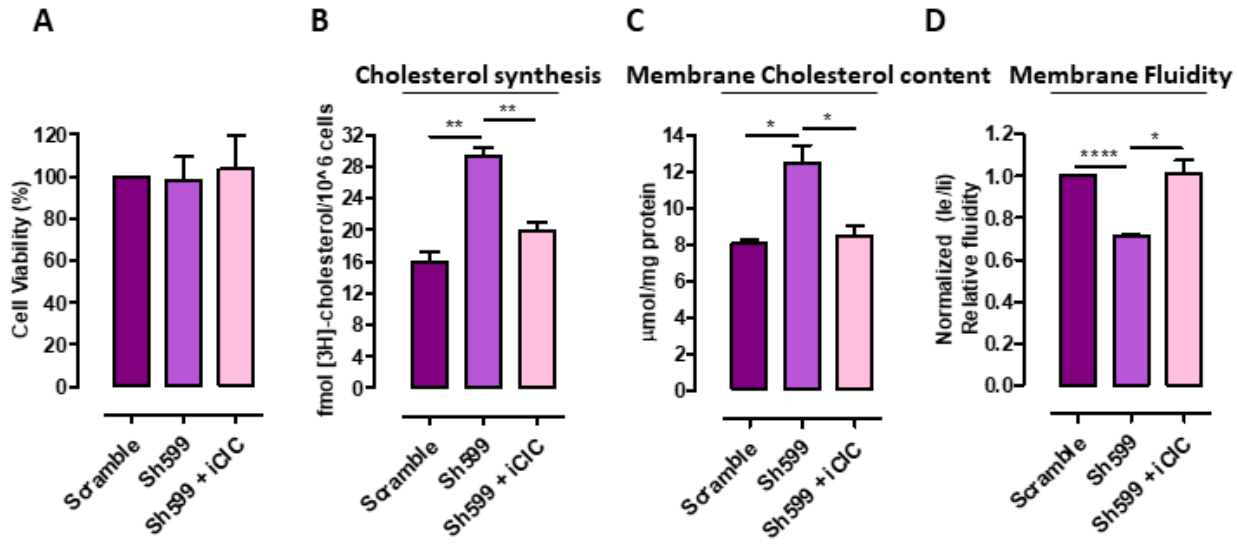

Figure 19. Cholesterol metabolism strictly depends on ALAS1-mediated succinyl-CoA consumption. [A] Cell viability was assessed thourgh crystal violet assay. Values are expressed as percentage (%) compared to control cells (Scramble). Data are expressed as mean ± SEM (N=3, n=4). Unpaired t-test was performed: *p<0.05, **p<0.01, ***p<0.001. **[B]** Rate *de novo* cholesterol synthesis is expressed as fmol of radiolabeled cholesterol over $1x10^6$ cells. Data are expressed as mean ± SEM (N=3, n=3). Unpaired t-test was performed: *p<0.05, **p<0.01, ***p<0.001. **[C]** Cholesterol content in plasma membrane is expressed as µmol/mg protein. Data are expressed as mean ± SEM (N=3). Unpaired t-test was performed: *p<0.05, **p<0.01, ***p<0.001. **[D]** Membrane fluidity is expressed as fold increase of normalized Ie/Ii (corresponding to eximer and monomer fluorescence, respectively) fluorescence over their respective controls. Data are expressed as mean ± SEM (N=3, n=3). Unpaired t-test was performed: *p<0.05, **p<0.01, ***p<0.001, ****p<0.0001. Scramble: control; Sh599: FLVCR1a-silenced cells; Sh599 + iCIC: FLVCR1a-silenced cells treated for 1h with 5 µM iCIC (rescue condition).

Taking together, these results suggest that, as previously hypothesized, [1] heme and cholesterol synthesis are tighly linked and that [2] membrane fluidity strictly depends on the correct balance between the above-mentioned cataplerotic pathways. To sum up, based on all these findings and on literature hints, we can so far postulate that, by modulating FLVCR1a levels, we can affect heme synthesis and, consequently, cholesterol synthesis. This metabolic adaptation is at the basis of the different membrane cholesterol content and, consequently, of the different membrane fluidity, observed following FLVCR1a levels modulation.

In vivo validation of the relationship between FLVCR1a, Cholesterol Synthesis and LSECs fenestration

What could be the biological relevance of these *in vitro* findings? What could be the implications for liver homeostasis and liver fibrosis?

To answer to these questions, we need to further dissect the role of FLVCR1a in LSECs *in vivo*.

Starting from these interesting *in vitro* data, as well as from the recent recognition of metabolism significance in healthy and dysfunctional ECs, we strongly believe that LSECs after chronic injury can rewire their metabolic profile (Fig. 21). Of interest, normal LSECs could have a high heme synthesis rate, at the expense of citrate efflux and cholesterol synthesis. This could allow LSECs to exhibit a fluid membrane, thus maintaining their fenestration. On the other hand, fibrotic LSECs could have a low heme synthesis rate, thus pumping cholesterol synthesis and, ultimately, stiffening the plasma membrane. For this reason, this metabolic adaptation could be the cause of LSEC defenestration in fibrotic livers. FLVCR1a could play a key role in dictating LSECs metabolic profile. In fact, normal LSECs express high levels of *Flvcr1a*, as shown by the microarray data analysis, thus pumping heme synthesis. On the contrary, we hypothesized that fibrotic LSECs could lose FLVCR1a expression, thus initiating all the above-mentioned metabolic alterations.

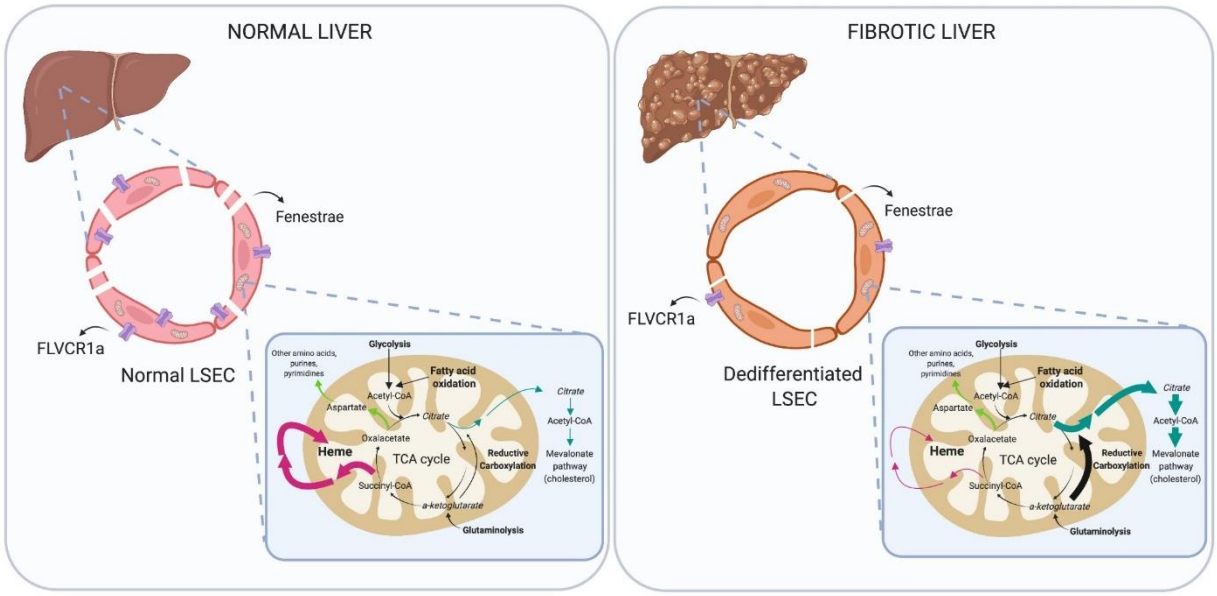

Figure 24. Working model. [A] Fibrotic dedifferentiated (i.e., without fenestrae) LSECs could downmodulate FLVCR1a, thus undergoing a metabolic rewiring. In particular, heme synthesis rate slows down, while citrate consumption and cholesterol synthesis take over. This metabolic rewiring could cause the consequent increase in cholesterol membrane content, thus compromising LSEC fenestration maintenance.

To validate this hypothesis, our collaborator in Barcelona (Prof. Jordi Gracia-Sancho) interrogated its RNA-seq data on LSECs derived from normal rats and from three different liver cirrhosis rat models (i.e., CCl4, TAA and BDL). We evaluated the expression of heme-related genes (Fig. 22). Unfortunately, probably due to sensitivity issue, *Flvrc1a* has not been detected. Nevertheless, we observed a clear downmodulation of heme synthesis-related genes in all the rat models but particularly in the CCl4 one.

A

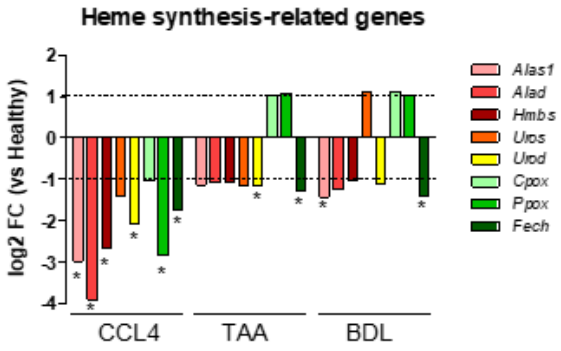

B

RAT LSECs (Log2 Fold Change vs Healthy)			
	CCL4	TAA	BDL
Alas1	-2,979*	-1,132	-1,433*
Alad	-3,906*	-1,079	-1,252
Hmbs	-2,678*	-1,076	-1,007
Uros	-1,407	-1,172	1,123
Urod	-2,075*	-1,169*	-1,111
Cpox	-1,034	1,042	1,124
Ppox	-2,830*	1,06	1,028
Fech	-1,726*	-1,273*	-1,403*

*** p-value≤0.05**

Figure 22. RNA-seq data on Normal and Cirrhotic rat LSECs. [A] Log2 Fold Change of heme synthesis-related genes expression in cirrhotic LSECs compared to healthy LSECs. Data are expressed as mean. Statistical analysis was performed: *p<0.05.

These results suggest that fibrotic/cirrhotic defenestrated LSECs exhibit a lower heme synthesis rate, compared to normal LSECs. Although further experiments are needed, as well as although enzyme mRNA expression levels do not necessarily reflect its metabolic activity, these RNA-seq data partially confirm our working model. This encourages us to perform other *in vivo* experiments (see Discussion and Future Perspectives).

DISCUSSION AND FUTURE PERSPECTIVES

CLDs and cirrhosis represent a major world health problem due to the high incidence and, most importantly, due to the lack of therapeutic treatments other than liver transplantation. This strongly highlights the urgent need to find alternative approaches.

Camussi's group has previously demonstrated that HLSCs exhibit anti-fibrotic and anti-inflammatory effects in a NASH mouse model, without differentiating into hepatocyte-like cells[40]. These results highlight the paracrine EVs-mediated regenerative effect of stem cells transplanted into an injured tissue, namely fatty and fibrotic liver. Starting from this hint, during my PhD, I assessed the therapeutic potential of HLSCs-derived EVs in an immunodeficient mouse model of cholestasis-induced liver fibrosis. Nowadays, multiple cholestasis-induced liver fibrosis mouse models exist and are employed to recapitulate, unravel and therapeutically target mechanisms of chronic biliary injury. One of the most commonly used models is the DDC feeding, which results in stereotypical histopathological alterations seen in human Primary Sclerosing Cholangitis. After having assessed the natural history of DDC diet-induced CLD in NSG mice, I started to evaluate *in vivo* the biological effect of HLSCs-derived EVs. To this purpose, I intravenously injected EVs into DDC intoxicated fibrotic mice by following three different treatment schedules. Briefly, biometrical, serum and expression data, as well as histological examination revealed that EVs-treated mice did not benefit from vesicles treatment. Indeed, fibrosis progression was not affected by EVs treatment in all the experiments.

However, it has been recently demonstrated that HLSCs-derived EVs exhibit anti-fibrotic effects in a NASH murine model[120]. Therefore, our data may seem controversial. Considering the route of administration (namely intravenous), we questioned wheter EVs are effectively capable of reaching fibrotic liver in our DDC mouse model. To this purpose, we performed IVIS biodistribution experiment by injecting fluorescent labeled-EVs. As expected, we observed that in healthy mice EVs preferentially accumulate into the liver, compared to the other organs (i.e., lung, spleen and kidney). This could be due to the physiological clearance activity of the liver. However, in DDC-intoxicated mice HLSCs-derived EVs are not able anymore to accumulate into the liver. Therefore, we can conclude that we were not able to appreciate any therapeutic effects in our DDC murine model because of the inability of HLSCs-derived EVs to reach the damaged liver and, consequently, to exert their potential anti-fibrotic and regenerative effects.
Although the regenerative properties of EVs have been extensively evaluated in different contexts, several issues related to their biogenesis, uptake, as well as biodistribution *in vivo* need still to be deeper assessed. Despite the underlying mechanisms are still not fully understood, in literature it has been widely accepted the concept that EVs can preferentially reach a damaged site. Unlike cells, EVs can't actively seek targets via signaling gradients. Therefore, it has been proposed that the passive accumulation seems the likely dominant distribution mechanism. Consistently, in inflammatory conditions injected EVs or nanoparticles may accumulate in inflamed tissue due to vascular leakiness[130]. For example, *in vivo* targeting of EVs to the heart is difficult because of the intact endothelial barrier; yet, if the tissue is infarcted the chance of infiltration will increase due to vascular leakiness[131]. Consistently, based on this consensus, Bruno S. *et al.* showed that the signal of fluorescent labeled-EVs was higher in fatty/fibrotic liver compared to the normal one. This biodistribution result confirmed that

EVs preferentially accumulate into a damage tissue, probably due to vascular leakiness. However, on the other hand, in literature it has been widely demonstrated that fibrotic liver exhibit a reduced vascular permeability and insufficient drug delivery[132,133]. This could be largely attributed to [1] the loss of sinusoidal fenestrae and [2] the perivascular deposition of extracellular matrix. Based on literature data, these phenomena happen very early in the DDC-induced liver fibrosis mouse model (i.e., 4 days of diet intoxication)[59]. For this reason, we believe that HLSCs-derived EVs do not infiltrate the fibrotic liver because of these "mechanical" vascular impedances. Therefore, our apparent controversial findings could be explained by considering the discrepancies between the two mouse models (our DDC *vs* their NASH). DDC intoxication induces a strong and fast fibrosis progression, while NASH mice, used in the above-mentioned paper, develop a slowly progressive CLD. It is likely that at the timing of their first injection mice did still not exhibit advanced fibrosis and sinusoidal capillarization. Consistently, the authors have could observe EVs accumulation into the liver and a EVs-mediated beneficial effect in terms of both fibrosis and inflammation. This strongly suggest that the major pathophysiological changes in the fibrotic liver, compromising EVs liver infiltration, were still not occured.

Considering all these hints, we aim at overcoming this "delivery issue", by designing "preventive" regimes. We are going to inject HLSCs-derived EVs in concomitance with DDC diet. Consistently, we will assess the capability of HLSCs-derived EVs to block or delay liver fibrosis onset. Although with this setting we will not anymore assess their therapeutic potential, we could at least get the proof-of-concept of the pro-regenerative and anti-fibrotic properties of HLSCs-derived EVs. Moreover, we are planning to evaluate the possible curative effect of HLSCs-derived EVs in other mouse models. In particular, we are going to use the knockout mice for Multidrug resistance protein 2 (*Mdr2 -/-*), spontaneously developing cholestasis, liver fibrosis and later hepatocellular carcinoma.

These results strongly highlight the importance of LSECs and sinusoidal vessels also in efficient drug delivery.

LSECs can be distinguished from all the other ECs in our body because of the presence of both "open" (i.e., without diaphragm) fenestrae and a disorganized/incomplete basement membrane. Interestingly, despite their high specialization, LSECs retain a considerable phenotypic and functional plasticity. In fact, loss of fenestration and deposition of an organized subendothelial basement membrane is called "capillarization"[47,52]. Nowadays, LSECs dedifferentiation or sinusoidal capillarization is considered a hallmark of liver fibrosis and cirrhosis, regardless of the underlying disease cause[57]. Importantly, over the last years it has been demonstrated that sinusoidal capillarization/LSECs dedifferentiation is implicated in the onset and progression of liver fibrosis. This central role in CLDs makes them an attractive and promising therapeutic target of new strategies that aim at restoring LSECs fenestration and, consequently, at interfering with CLD progression[57].
Based on the encouraging data about the impact of heme exporter FLVCR1a loss and heme metabolism dysregulation in ECs on microvascular network formation during embryonic development[80,96], we decided to dissect its role in quiescent adult ECs and specifically in LSECs. Importantly, the bioinformatic analysis of a public microarray dataset, highlighting the molecular heterogeneity of murine microvascular ECs, revealed that *Flvcr1a* is particularly

enriched in LSECs, compared to the other tissue-specific ECs. Starting from this important hint, we started questioning about the possible involvement of FLVCR1a in the maintenance of fenestration.

Despite the first observation of LSECs fenestration dates to 1970s[46], the molecular and structural mechanisms underlying the formation, maintenance and dynamic regulation of LSECs fenestrae are still elusive. This is because one of the major challenges in studying LSECs biology is related to technical and methodological limitations. In particular, due to the small diameter of these pores (namely 100-200 nm), nowadays, the gold standard method to detect and measure LSECs fenestrae is Scanning Electron Microscopy analysis (SEM), both *in vitro* and *in vivo*. By treating Sk-Hep1 cells with cytochalasin and antimycin (i.e., well-known positive and negative regulators of fenestrae, respectively[126]), we demonstrated that membrane fluidity could be a reliable indirect paramenter of LSECs fenestration[124,125]. It has been proposed the hypothesis that fenestrae originate from a process of membrane invagination and, consequently, from its fusion with basolateral membrane. Consistently, the physical-chemical properties of plasma membrane are extremely important. In particular, a reduced membrane tension leads to membrane invaginations, whereas an increased membrane tension hampers these invaginations[124,125]. We measured membrane fluidity, as an indirect parameter of fenestration, upon FLVCR1a modulation. The results suggest that FLVCR1a positively regulates membrane fluidity, thus allowing us to speculate that FLVCR1a can positively regulate fenestrae formation and/or maintenance. This is perfectly in line with the observed high expression of *Flvcr1a* in LSECs, compared to the other tissue-specific ECs. Although these results are quite suggestive of a capillarization upon FLVCR1a silencing, the gene expression analysis of genes known to vary according to the status of the sinusoidal cells could further support and corroborate our data.

Cholesterol plays a key role in regulating membrane tension and fenestrae formation. Indeed, cholesterol depletion and cholesterol accumulation in plasma membrane leads to an increase and decrease in the number of fenestrations, respectively[124,125]. For this reason, we then assessed membrane cholesterol content in Sk-Hep1 cells upon FLVCR1a modulation. Briefly, we observed that FLVCR1a levels inversely correlate with membrane cholesterol content, thus suggesting that FLVCR1a may regulate the membrane fluidity by affecting its cholesterol content.

Heme is an essential co-factor in multiple biological processes. Nevetherless, excess free-heme is highly toxic due to its ability to promote ROS production, thus ultimately leading to apoptosis. Thus, heme metabolism needs to be finely regulated[93]. Fiorito V. *et al.* recently showed that in colorectal cancer cells exists a heme exporter-synthesis axis aiming at maintaining normal and physiological intracellular heme levels (under revision). In particular, a high heme exporter activity leads to a high heme synthesis and, on the contrary, a low heme exporter activity leads to a low heme synthesis. Of interest, both FLVCR1a-overexpressing and FLVCR1a-silenced Sk-Hep1 cell lines did not exhibit differences in terms of both heme and ROS levels, compared to their respective controls, as well as in terms of cell viability. We can speculate that this axis is a general rather than specific mechanism of colorectal cancer cells.

Mechanistically, we demonstrated that heme synthesis and cholesterol synthesis are tighly linked one to each other. Of interest, FLVCR1a-overexpressing cells and FLVCR1a-silenced cells exhibited a lower and higher cholesterol synthesis rate, respectively, compared to their

controls. Heme synthesis and cholesterol synthesis are both considered cataplerotic pathway. In fact, succinyl-CoA and citrate are TCA intermediates that leave the cycle to be converted (through several enzymatic reactions) to heme and cholesterol, respectively. To explain the balance between cataplerosis and anaplerosis, TCA cycle has been previously compared to a traffic circle on a busy highway. This means that the flow of cars into the circle must be balanced by the flow out or the entire traffic pattern will be interrupted with disastrous consequences[127]. However, also the several cataplerotic pathways need to be finely balanced. In this view, the cataplerotic pathways act more as road branches starting from the traffic circle. If the main road is closed (e.g., in FLVCR1a-silenced cells the main road is ALAS1-mediated succinyl-CoA consumption and heme synthesis), the cars have to flow out from the traffic circle through another secondary road (e.g., in FLVCR1a-silenced cells the secondary road is citrate efflux and its conversion into cholesterol). By performing rescue experiments with ALA and iCIC in FLVCR1a-overexpressing cells and FLVCR1a-silenced cells, respectively, we demonstrated that heme synthesis rate dictates citrate efflux and its conversion in cholesterol. Overall, we observed that this metabolic adaptation, consequently, has an impact on both membrane cholesterol content and membrane fluidity.

Over the last years, it has been demonstrated that normal ECs and dysfunctional/diseased ECs exhibit a different metabolic profile, thus suggesting that metabolism could be a major determinat of ECs biology and, consequently, of the whole pathological process[79]. As a consequence, novel "EC metabolism-centric" therapeutic avenues are recently proposed. Besides the most common studied metabolic pathways (e.g., glycolysis and glutaminolysis), heme metabolism, which has been overlooked for long time, is currently getting more and more attention and seems to be tighly connected to the other pathways[80–83]. However, so far the molecular profile of differentiated and dedifferentiated LSECs has never been extensively explored[84]. Overall, based on our *in vitro* experiments and RNA-seq data, showing a clear downmodulation of heme synthesis-related genes in fibrotic/cirrhotic defenestrated LSECs, we can state that normal LSECs (i.e., with fenestrae) have a different metabolic signature compared to dedifferentiated ones (i.e., without fenestrae). In particular, normal LSECs express high levels of FLVCR1a, thus pumping heme synthesis at the expense of cholesterol. This metabolic profile could allow LSECs to exhibit a fluid membrane and to maintain their fenestration. On the contrary, dedifferentiated LSECs could have lower levels of FLVCR1a, thus activating all the above-mentioned metabolic rewiring. Consequently, membrane cholesterol content increases and LSECs lose their fenestration. An hint supporting our working model comes from the literature[134]. Microarray analysis has been performed on LSECs derived from CDAA diet-induced NASH mice *versus* healthy mice. GSEA analysis showed that "Cholesterol Homeostasis" is activated in fibrotic LSECs, compared to normal LSECs, thus supporting the notion that cholesterol synthesis could be positively affected in dedifferentiated LSECs[134]. Overall, by modulating heme/cholesterol metabolism, we could affect LSECs fenestration. We strongly believe that both heme or cholesterol metabolism players could be a plausible target to restore LSECs fenestration, thus hopefully prevent liver fibrosis progression and improve drug delivery.

Statins represent a heterogeneous group of molecules that inhibit the activity of HydroxyMethylGlutaryl-Coenzyme A (HMG-CoA) reductase, a key enzyme in the synthesis of

cholesterol. Thus, statins are used worldwide for the management of dyslipidaemia[135]. However, in addition to lowering cholesterol levels, statins have pleiotropic effects, particularly anti-inflammatory, anti-angiogenic, as well as anti-fibrotic, that may be beneficial in some chronic inflammatory conditions. Consistently, over the recent years studies in animal models of liver diseases have shown that statins reduce liver fibrosis, improve endothelial dysfunction and decrease portal pressure[136]. However, due to its severe side effects, statins are not still recommended for use in clinical practice. As previously stated, CLDs, independently from their aetiologies, are characterized by endothelial dysfunction that ultimately leads to the development of portal hypertension. This is mostly attributed to an imbalance in the vascular tone-regulating pathways, showing a shift towards vasoconstriction. All these pathways may be modulated by statins[137–140]. Moreover, it has been shown that statins treatment restores LSECs differentiation in a NASH mouse model[141]. Surprisingly, despite it has been proven that statins improve endothelial phenotype, there are no information on the effect of statins on LSECs cholesterol metabolism.

Based on our *in vitro* data, the final goal is to propose heme metabolism as a plausible target in restoring LSECs differentiation and in slowing down liver fibrosis progression. To this end, we still have to confirm and strengthen our working model, as well as to perform further *in vivo* experiments. Consistently, we have a lot of open questions: [1] do endothelial-specific *Flvcr1a* knock-out mice undergo LSECs dedifferentiation and spontaneously develop liver fibrosis?, [2] are endothelial-specific *Flvcr1a* knock-out mice more susceptible to pro-fibrogenic stimuli?, [3] during sinusoidal capillarization, do LSECs downregulate *Flvcr1a*? and [4] if yes, is the overexpression of FLVCR1a in “fibrotic” LSECs sufficient to restore fenestrae and to prevent the progression of liver fibrosis in mice?

MATERIAL AND METHODS

In vivo murine model

Animal studies were conducted in accordance with the National Institute of Health Guide for the Care and Use of Laboratory Animals. All procedures were approved by the Italian Health Ministry (Ethical number of the study: CC652.84). Mice were given *ad libitum* access to food and water.

To assess its natural history in immunocompromised mice, we induced Cholestasis-induced Liver Fibrosis by feeding male NSG mice (6-8 weeks old) with 0,1% DDC-supplemented diet and by sacrifing them at different time points, namely 4, 6, 8, 10, 12, 14 and 16 weeks (N=3 for each time point). This "experimental group" was compared to standard diet-fed "control" mice (Fig. 7, A). In particular, to exclude age-related changes in the analyzed parameters, we used three different groups of control mice, sacrified at three specific time points (8, 12, 16 weeks) with their age-matched experimental mice (N=9, N=3 for each control group). Moreover, to assess the reversibility of the cholestatic and fibrotic phenotype observed in 8 weeks DDC-fed mice, we allowed an additional group of animals (N=3) to return to the standard diet for 2 other weeks ("recovery group").

To evaluate the anti-fibrotic properties of HLSCs-derived EVs, mice with establised liver fibrosis were intravenously (tail vein) injected with EVs. Of interest, it should be noted that there are a lot of variables, which should be taken into account. For example, the timing at which start and end the treatment, the dose of EVs to be administrated, as well as the weekly frequency of injections. Therefore, based on all these variables, we designed and carried out three different therapeutic regimens (Fig. 10). In particular, in the first two regimens different amount of EVs were injected once a week, starting after 4 weeks of DDC diet, when fibrosis and cholestasis were established (Fig. 10, A-B). Each mouse received a total of four EVs injections. Two doses were tested (Fig. 10, A-B), namely $1x10^8$ EVs/mouse/injection (N=6) and $2,5x10^9$ EVs/mouse/ injection (N=3). In the third experiment, instead, we injected $2,5x10^9$ EVs twice a week, starting at 2 weeks of DDC diet (N=4). Also in this case, each mouse received a total of four EVs injections, but distributed in only 2 weeks (Fig. 10, C). Control DDC-induced fibrotic mice (N=6 in the first, N=3 in the second and N=4 in the third experiment) were injected with vehicle alone (PBS).

At the end of each experiment, all mice were appropriately sacrified and blood and liver were harvested for subsequent biochemical, histologic and molecular analysis.

HLSCs-derived EVs purification and characterization

As previously mentioned (see Aims), we collaborated with Prof. Camussi G. Therefore, in all the experiments we used HLSCs-derived vesicles produced by Camussi's group. Every batch of EVs preparation was accurately checked before being used, as previously reported, through Nanoparticle Tracking Analysis (NTA), bead-based flow citometry and electron microscopy analysis[120].

Liver sampling

One of the most debated issue, related to the interpretation and comparison of the inter- and intra-laboratories obtained findings, is the harvesting and processing of the liver. For this

reason, we followed the previously reported guidelines[106], thus setting-up and carrying out in all the experiments a standardized work-up for mouse liver tissue (Fig. 23). For example, since it has been reported that there are significant morphological and physiological differences between the liver lobes (such as the degree of ductular reaction, as well as the size of bile ducts), we have always collected and used for a specific application the same liver lobe from all the analyzed mice. Moreover, since most biological processed have a pronounced circadian rhythm, liver have always been harvested in the morning (between 8:00 a.m. and 12:00 noon).

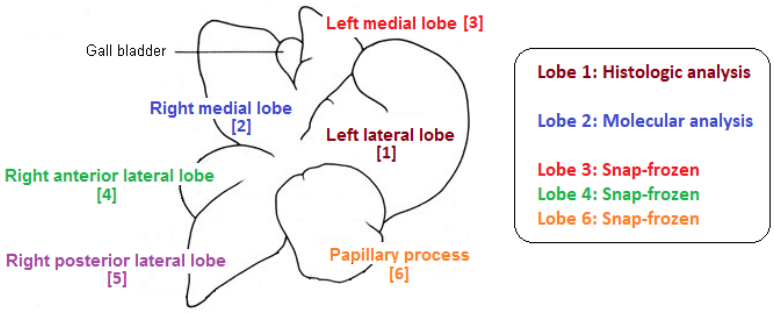

Figure 23. Liver sampling. Upon harvesting, liver lobes were dissected and opportunely "sorted" for the different applications. Lobe 1 was immediately fixed in formalin and further processed for histologic analysis. Lobe 2 was sanp-frozen and stocked at -80 °C until RNA extraction for molecular analysis. Lobe 3, 4 and 6 were all snap-frozen and stocked at -80 °C for further analysis performed by the other Companies in Piedmont, involved in this project.

Serum tests

Blood samples were collected (and later kept on ice) through heart puncture from mice under deep terminal anaesthesia. To promote blood coagulation, the samples were incubated at 37°C for 10 minutes and later were centrifuged at 5000xg for 10 minutes at 4°C. The supernatant, namely the serum, was recovered and stocked at -80 °C until use for subsequent analysis. Serum biochemical analysis (AST, ALT, and ALP expressed as U/L, as well as Albumin expressed as g/dL) have been performed at the Department of Veterinary Science (Unito), thanks to the collaboration with Prof. Miniscalco Barbara.

Histologic analysis

As previously discussed, we standardized our work-up for mouse liver tissue and we always used the "Lobe 1" to perform histologic analysis.
Collagen deposition was assessed by performing PicroSirius Red (PSR) stain on formalin-fixed paraffin-embedded liver sections (5 µm-thick), as previously described (www.ihcworld.com). The PSR stain (also called "Sirius red" stain) is one of the best understood histochemical techniques able to selectively highlight collagen networks. In particular, in bright-field microscopy collagen is red on a pale yellow background. Nuclei, if stained, are ideally black but may often be grey or brown.
Briefly, paraffin liver sections were appropriately dewaxed, hydrated and were incubated in picro-sirius red solution at least 1h. Then, slices were quickly washed in 0,5% acidified water, hydrated, cleared in xylene and mounted. Images were acquired on bright-field microsope Olympus BX41 with 2,5X or 4X objectives, to obtain "qualitative" or "quantitative" information, respectively. In fact, in the latter case, to assess the (potential) anti-fibrotic effect of HLSCs-derived EVs, quantitative morphometric measurements were performed. Consistently, liver fibrosis was quantified by [1] measuring collagenous fibrotic area (stained in red) and [2] normalizing it to the respective total area, from which area corresponding to blood vessels

lumen was previously substracted. Therefore, data are expressed as percentage (%) of red area over total (without vessels) area. We analyzed at least 5 random fields/section/mouse by using ImageJ software and a custom "Color Deconvolution" method.

In vivo bio-distribution of HLSCs-derived EVs

Age-matched mice fed for 2 weeks with 0,1% DDC-supplemented diet and healthy mice were intravenously (tail vein) injected with $1,5x10^{10}$ DiD (fluorescent)-labeled EVs and their localization were monitored by optical imaging (OI) (N=3/group). It is further noteworthy that, due to technical limitations related to instrument sensitivity, we injected a higher quantity of EVs, compared to those used in the previous three "biological" experiments. In parallel, to assess and substract the organs autofluorescence signal, in other age-matched DDC- and standard diet-fed mice (N=1/group, "blank mice") we did not inject DiD-fluorescent EVs but PBS, thus measuring the background fluorescent signal of their dissected organs. At the end of the experiment (3h post-injection), liver, lung, kidneys and spleen were harvested and immediately imaged with IVIS 200 small animal imaging system (PerkinElmer) using excitation filter at 640 nm and emission filter at 700 nm. The fluorescence signal was quantified in Region Of Interest (ROI) draw freehand. Fluorescence emission was normalized to photons per second per centimetre squared per steradian (p/sec/cm^2/sr), as previously described[121]. The mean fluorescence of each tissue sample was obtained by subtracting the fluorescence intensity of corresponding tissue from the blank mouse. Data are expresses as radiance. Images were acquired and analyzed using Living Image 4.0 software (PerkinElmer).

Cell culture

In vitro assays, concerning the biological role of FLVCR1a in LSECs, were performed on a human cell line resembling LSECs, the so-called Sk-Hep1. Sk-Hep1 cell line was purchased by the American Type Culture Collection (ATCC) and was propagated in DMEM medium (Gibco) with 10% FBS (Gibco), 100 U/ml Penicillin and 100 µg/ml Streptomycin (Gibco). Sk-Hep1 cells were used up to passages 20-25 and were maintained at 37 °C under 5% CO_2 atmosphere. Moreover, they were tested for mycoplasma contamination regularly.
To test the utility of membrane fluidity assay as indirect parameter of LSECs fenestration, cells were treated for 1h with 2 µM Cythocalasin D (C2618, Sigma) or 1 µg/ml Antimycin A (A8674, Sigma)[126]. To "shut down" ALAS1-mediated succinyl-CoA utilization, FLVCR1a-overexpressing cells were trated for 24h with 5 mM 5-AminoLevulinic Acid hydrochloride (A3785, Sigma). FLVCR1a-silenced cells were treated for 1h with 5 uM iCIC (SML0068, Sigma).

FLVCR1a silencing and overexpression

A shRNA against the first exon of human *FLVCR1* gene (RHS4533-NM_014053, Dharmacon) was used to specifically down-regulate FLVCR1a isoform expression, as previously reported[80]. While pLKO.1 vectors were purchased, human FLVCR1a-myc has been previously cloned into pLVX-puro vector by Prof. Tolosano's group. The lentiviruses [1] pLKO.1-sh599 (expressing the shRNA specific for *FLVCR1a*), [2] pLKO.1-scr (expressing a "scramble" shRNA as control), [3] pLVX-FLVCR1a-myc and [4] pLVX-empty as control were produced in HEK293FT cells. Following lentiviral infection, Sk-Hep1 cells were selected with 1,25 µg/ml puromycin and later constantly maintained in 1 µg/ml puromycin containing cell medium (with puromycin renewal every 48h).

Measurement of intracellular heme content

Intracellular heme content was measured using a fluorescence assay, as previously reported[142]. This assay is essentially based on the fluorescent properties of PPIX.
Briefly, 240.000 cells were plated into 6-well plate and were collected by scraping and lysed in TBS-1% Triton-X-100 after 48h (comprising also of the 24h of ALA treatment, when required). Following an incubation of 15 min on ice, cell lysates were assayed for protein concentration using the Bio-Rad protein assay method (Biorad). Then, 500 µl of the 2 M Oxalic Acid (OA) solution were added to 50 µl of 1 µg/µl proteins in PBS. Samples in OA were heated at 95 °C for 30 min to trigger the removal of iron from heme, thus obtaining the heme-derived fluorescent PPIX. Fluorescence (Excitation wavelenght 405 nm; Emission wavelenghts 580-640 nm) was assessed on a Glomax Multi Detection System (Promega Corporation) by using black optical 96-well plate. However, this measured fluorescent signal comprises of both heme-derived and endogenous PPIX fluorescence. For this reason, the endogenous PPIX content was assessed and substracted by measuring in parallel the fluorescence of unheated, namely incubated 30 min not at 95 °C but at at room temperature, samples in OA. Data are expressed as a fold increase over the calibrator sample(s). Heme assay was performed in technical duplicate in three indipendent experiments.

Measurement of intracellular ROS content

Intracellular ROS content was measured using a fluorescence assay, as previously reported[80]. This assay requires the oxidant-sensitive fluorescent dye H2DCFDA (D6883, Sigma).
Briefly, 240.000 cells were plated into 6-well plate and, after 48h (comprising also of the 24h of ALA treatment, when required), were washed with PBS and incubated with 10 µM H2DCFDA probe in serum-free cell medium for 50 min at 37 °C under 5% CO2 atmosphere. Then, cells were washed twice with PBS, collected by scraping and lysed in TBS-1% Triton-X-100. Following an incubation of 15 min on ice, cell lysates were assayed for protein concentration using the Bio-Rad protein assay method (Biorad). Then, the fluorescence of 200 µl of 0,25 µg/µl proteins in PBS (Excitation wavelenght 485 nm; Emission wavelenghts 500-550 nm) was assessed on a Glomax Multi Detection System (Promega Corporation) by using black optical 96-well plate. Data are expressed as a fold increase over the calibrator sample(s). ROS assay was performed in technical duplicate in three indipendent experiments.

Crystal Viability assay

The staining of adherent cells via crystal violet is commonly used in molecular biology to investigate cell viability[143]. The disadvantage of the crystal violet assay is that this assay can't distinguish between cell death's and cell proliferation's contribution.
To assess the impact of FLVCR1a levels modulation on cell viability, 40.000 Sk-Hep1 were plated in 24-well plate and every 24h (up to 96h) were processed. Briefly, the medium was aspired and cell were kindly washed once with 500 µl PBS. After washing, 250 µl of crystal violet solution was added in each well and the plate was incubated 30 min at room temperature. Afterward, the plate was washed 5 times (500 µl/well/wash) with tap water and was let it dried for at least 2h at room temperature with open lid until further processing. Before moving to the

spectrophotometric measurements, images of plates were captured using a scanner. Afterward, to elute the dye, 300 µl of 10% acetic acid was added in each well and the plate was incubated 30 min in gentle continuous agitation. The Optical Density (OD, 560 nm) of each well was measured on a Glomax Multi Detection System (Promega Corporation). Data are expressed as fold increase at 1, 2, 3 days over day 0 (namely the first measurement 24h after plating). Crystal violet assay was performed in technical quadruplicate in three indipendent experiments.

To monitor the acute toxicity of 5 mM ALA treatment, 80.000 Sk-Hep1 cells were plated in 24-well plate. After 24h from plating, a plate was processed (day 0) and the other one was treated with ALA and processed after further 24h (day 1). The "day 1 OD" were normalized to their respective "day 0 OD". Viability data are expressed as percentage (%) over empty cells, which are used as calibrator. Crystal violet assay was performed in technical quadruplicate in three indipendent experiments. The same approach has been used to monitor the acute toxicity of 5 µM iCIC treatment.

Membrane Fluidity assay

Membrane fluidity assay relies on the utilization of a lipophilic fluorescent probe, that exhibits changes in their spectral properties in a membrane fluidity-dependent manner. Alterations in lipid packing affect short range lateral diffusion of membrane-bound fluorophore. Consistently, a "fluid membrane" allow the spatial interaction of the lipophilic probe, thus leading to eximer formation, whereas a "rigid membrane" do not. When eximers form, the emission spectrum of the probe shifts dramatically to the red (longer wavelength). By measuring the ratio of monomer (Ie, emission wavelenght ~372 nm) to eximer (Ii, emission wavelenght ~470 nm) fluorescence, a quantitative monitoring of the membrane fluidity can be attained.

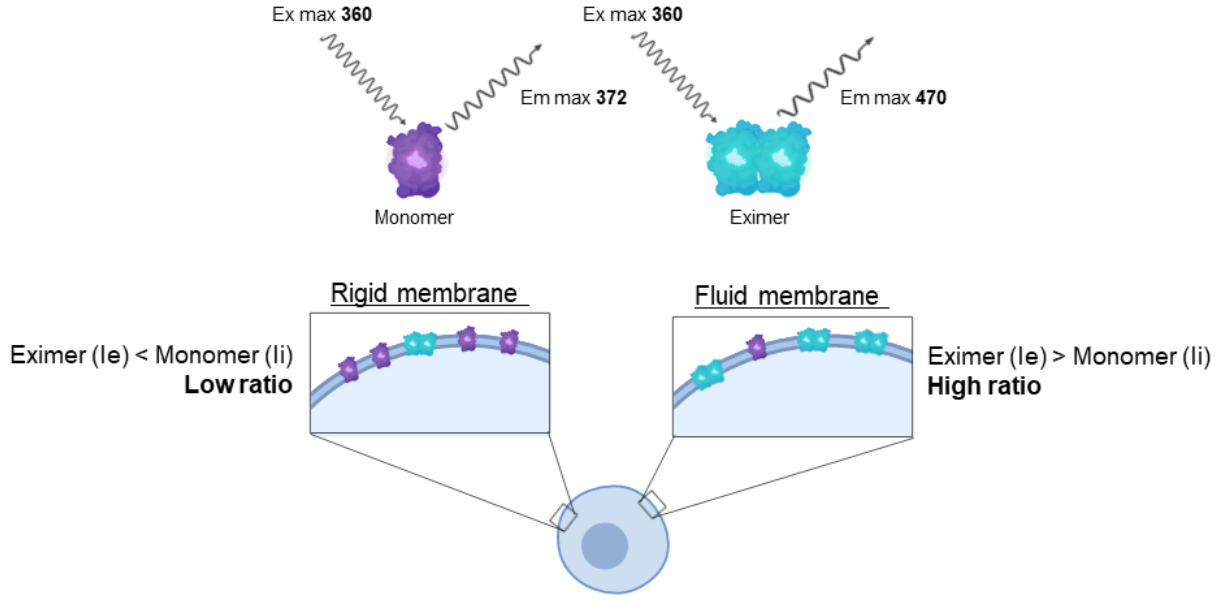

Membrane fluidity was measured by Prof. Riganti using a membrane fluidity kit (#M0271, Marker Gene Technologies), according to the manufacturer's protocol. Membrane fluidity assay was performed in technical triplicate in three indipendent experiments.

Membrane cholesterol content

Membrane were purified by following an-Abcam recommended subcellular fractionation protocol with some modifications (www.abcam.com). Briefly, 1.440.000 Sk-Hep1 cells were plated in 100cm dish and after 48h (comprising also of the 24h of ALA treatment, when required) were collected and lysed in 500 µl of Fractionation Buffer* by scraping (Table 2). Following an incubation of 15 min on ice, lysis was further promoted by passing the lysates through 25 gauge needle 10 times and by keeping them on ice for further 20 min. To remove nuclei and mithocondria, lysates were centrifuged at 10.000xg for 5 min at 4 °C. The supernatant was subsequently ultracentrifuged (Beckman Coulter's, rotor 70Ti) at 100.000xg for 1h at 4 °C. The supernatant, namely cytoplasm fraction, was discarded, whereas pellet, namely membrane fraction, was resuspended in 200 µl of PBS and stocked at -80 °C until further processing.
Prof. Riganti Chiara measured cholesterol concentration with an enzymatic colorimetric assay kit (OSR6516, Olympus System Reagent, Olympus Europe Holding GmbH, Hamburg, Germany), as previously reported[144]. Briefly, the absorbance was measured at 540/600 nm by an Olympus Analyzers spectrophotometer (Olympus Europe Holding GmbH). A 50 µL aliquot of membrane extracts was used to determine the protein content with the BCA kit. The results are expressed as µmol cholesterol/mg membrane proteins, according to a previously prepared titration curve. Membrane cholesterol assay was performed in three indipendent experiments.

Chemical	Final concentration
HEPES (pH 7,4)	20 mM
KCl	10 mM
$MgCl_2$	2 mM
EDTA	1 mM
EGTA	1 mM
DTT*	1 mM
Phosphatases Inhibitors cocktail 25X (Roche)*	-

*Added just before use

Table 2. Fractionation Buffer recipe.

De novo synthesis of cholesterol

Prof. Riganti Chiara performed a dynamic analysis of cholesterol synthesis rate by incubating cells with a radiolabeled cholesterol precursor, as previously reported[139]. Briefly, 240.000 Sk-Hep1 cells were plated in 6-well plate and the following day were incubated for 24h with 1 µCi/mL [^{3}H]-acetate (Amersham Bioscience). Afterward, cells were washed with PBS and transferred to glass microcentrifuge tubes. The intracellular synthesis of radiolabeled cholesterol was measured by the methanol/hexane extraction method, followed by thin layer chromatography. Standard solutions of cholesterol (Sigma Chemical Co.) were also loaded on the chromatography gel. After the separation, the gel was exposed to an iodine-saturated

atmosphere. Each spot was cut and solubilised and the radioactivity incorporated measured by liquid scintillation counting (Ultima Gold, PerkinElmer). The results are expressed as fmol/10^6 cells, according to the titration curve previously obtained. Dynamic synthesis cholesterol assay was performed in technical triplicate in three indipendent experiments.

RNA extraction and real-time PCR analysis

Total RNA was extracted from (snap-frozen Lobe 2) liver and cell samples using TRIzol™ reagent, according to the manifacturer's instructions (Invitrogen). For quantitative real-time polymerase chain reaction (qRT-PCR), 1 µg total RNA was retro-transcribed into complementary DNA (cDNA) using High-Capacity cDNA Reverse Transcription Kit (Applied Biosystems). qRT-PCR was carried out using Platinum™ Quantitative PCR SuperMix-UDG w/ROX (Applied Biosystems) and was performed on 7900HT Fast Real-Time PCR System (Applied Biosystems) or on QuantStudio 6 Flex Real-Time PCR System (Applied Biosystems) with 96-well or 384-well plate, respectively. Primers and probes were designed using the Universal ProbeLibrary Assay Design Center software (www. lifescience.roche.com). For FLVCR1a and FLVCR1b, specific primers and "common" probe were designed using Primer Express Software Version 3.0 (Applied Biosystems). Analysis was performed using the $2^{-\Delta\Delta Ct}$ method. Therefore, relative transcript abundance, normalized to 18s mRNA expression, is expressed as a fold increase over the calibrator sample(s).

The sequences of the primers and the respective probe are listed in the Table 3.

Gene	Left primer (sequence 5'-3')	Right primer (sequence 5'-3')	Probe (Roche)
m*Mmp2*	AACTTTGAGAAGGATGGCAAGT	TGCCACCCATGGTAAACAA	#29
m*Mmp9*	ACGACATAGACGGCATCCA	GCTGTGGTTCAGTTGTGGTG	#19
m*Timp1*	GCAAAGAGCTTTCTCAAAGACC	AGGGATAGATAAACAGGGAAACACT	#76
m*Timp2*	TTTTGCAATGCAGACGTAGTG	GGAATCCACCTCCTTCTCG	#21
m*Tgfß*	TGGAGCAACATGTGGAACTC	GTCAGCAGCCGGTTACCA	#72
m*Tweak*	CAGGATGGAGCACAAGCAG	GGCTGGAGCTGTTGATTTTG	#103
m*Fn14*	ATTCGGCTTGGTGTTGATG	CCATGCACTTGTCGAGGTC	#1
h*ALAS1*			
h*FLVCR1a*	TTGGGCCCAAAGAGGTGTC	GCCAGGAGATTTGTGTCATTCTG	Custom probe
h*FLVCR1b*	TCCTCTTTATGTTCTGTTAATTGCCA	GCCAGGAGATTTGTGTCATTCTG	Custom probe

Table 3. Sequences of the primers and the respective probe.

Statistics

Data analysis were performed using GraphPad Prism 8.3.1. Results are expressed as mean ± SEM. Statistical analysis were performed by employing the student's t-test. A p value of <0.05 was considered statistically significant.

BIBLIOGRAPHY

1. Moon, A. M., Singal, A. G. & Tapper, E. B. Contemporary Epidemiology of Chronic Liver Disease and Cirrhosis. *Clin. Gastroenterol. Hepatol.* (2019). doi:10.1016/j.cgh.2019.07.060

2. Asrani, S. K., Devarbhavi, H., Eaton, J. & Kamath, P. S. Burden of liver diseases in the world. *Journal of Hepatology* **70,** 151–171 (2019).

3. Baranova, A., Lal, P., Birerdinc, A. & Younossi, Z. M. Non-Invasive markers for hepatic fibrosis. *BMC Gastroenterology* **11,** (2011).

4. Wynn, T. A. Common and unique mechanisms regulate fibrosis in various fibroproliferative diseases. *Journal of Clinical Investigation* **117,** 524–529 (2007).

5. Ellis, E. L. & Mann, D. A. Clinical evidence for the regression of liver fibrosis. *Journal of Hepatology* **56,** 1171–1180 (2012).

6. Pellicoro, A., Ramachandran, P., Iredale, J. P. & Fallowfield, J. A. Liver fibrosis and repair: Immune regulation of wound healing in a solid organ. *Nature Reviews Immunology* **14,** 181–194 (2014).

7. Hirschfield, G. M., Heathcote, E. J. & Gershwin, M. E. Pathogenesis of cholestatic liver disease and therapeutic approaches. *Gastroenterology* **139,** 1481–1496 (2010).

8. Abshagen, K. *et al.* Pathobiochemical signatures of cholestatic liver disease in bile duct ligated mice. *BMC Syst. Biol.* **9,** (2015).

9. Jakubowski, A. *et al.* TWEAK induces liver progenitor cell proliferation. *J. Clin. Invest.* **115,** 2330–2340 (2005).

10. Dwyer, B. J., Olynyk, J. K., Ramm, G. A. & Tirnitz-Parker, J. E. E. TWEAK and LTß signaling during chronic liver disease. *Frontiers in Immunology* **5,** (2014).

11. Bravo, E., D'Amore, E., Ciaffoni, F. & Mammola, C. L. Evaluation of the spontaneous reversibility of carbon tetrachloride-induced liver cirrhosis in rabbits. *Lab. Anim.* **46,** 122–128 (2012).

12. Adiwinatapawitan, J. Exploring the Most Promising Stem Cell Therapy in Liver Failure: A Systematic Review. *Stem Cells Int.* **2019,** (2019).

13. Kang, S. H., Kim, M. Y., Eom, Y. W. & Baik, S. K. Mesenchymal Stem Cells for the Treatment of Liver Disease: Present and Perspectives. *Gut Liver* (2019). doi:10.5009/gnl18412

14. Amariglio, N. *et al.* Donor-derived brain tumor following neural stem cell transplantation in an ataxia telangiectasia patient. *PLoS Med.* **6,** 0221–0231 (2009).

15. Werbowetski-Ogilvie, T. E. *et al.* Characterization of human embryonic stem cells with features of neoplastic progression. *Nat. Biotechnol.* **27,** 91–97 (2009).

16. Aguilar, S. *et al.* Murine but Not Human Mesenchymal Stem Cells Generate Osteosarcoma-Like Lesions in the Lung. *Stem Cells* **25,** 1586–1594 (2007).

17. Breitbach, M. *et al.* Potential risks of bone marrow cell transplantation into infarcted hearts. *Blood* **110,** 1362–1369 (2007).

18. Kunter, U. *et al.* Mesenchymal stem cells prevent progressive experimental renal failure but maldifferentiate into glomerular adipocytes. *J. Am. Soc. Nephrol.* **18,** 1754–1764 (2007).

19. Cernigliaro, V. *et al.* Evolving Cell-Based and Cell-Free Clinical Strategies for Treating Severe Human Liver Diseases. *Cells* **9,** 386 (2020).

20. Baraniak, P. R. & McDevitt, T. C. Stem cell paracrine actions and tissue regeneration.

Regenerative Medicine **5,** 121–143 (2010).

21. Raposo, G. & Stahl, P. D. Extracellular vesicles: a new communication paradigm? *Nature Reviews Molecular Cell Biology* **20,** 509–510 (2019).

22. Lee, J.-K. Extracellular Vesicles as an Emerging Paradigm of Cell-to-Cell Communication in Stem Cell Biology. *J. Stem Cell Res. Ther.* **4,** (2014).

23. Tetta, C., Ghigo, E., Silengo, L., Deregibus, M. C. & Camussi, G. Extracellular vesicles as an emerging mechanism of cell-to-cell communication. *Endocrine* **44,** 11–19 (2013).

24. Devhare, P. B. & Ray, R. B. Extracellular vesicles: Novel mediator for cell to cell communications in liver pathogenesis. *Molecular Aspects of Medicine* **60,** 115–122 (2018).

25. Ratajczak, M. Z. *et al.* Pivotal role of paracrine effects in stem cell therapies in regenerative medicine: Can we translate stem cell-secreted paracrine factors and microvesicles into better therapeutic strategies. *Leukemia* **26,** 1166–1173 (2012).

26. Quesenberry, P. J., Dooner, M. S. & Aliotta, J. M. Stem cell plasticity revisited: The continuum marrow model and phenotypic changes mediated by microvesicles. *Experimental Hematology* **38,** 581–592 (2010).

27. Camussi, G., Deregibus, M. C. & Tetta, C. Paracrine/endocrine mechanism of stem cells on kidney repair: Role of microvesicle-mediated transfer of genetic information. *Current Opinion in Nephrology and Hypertension* **19,** 7–12 (2010).

28. Bruno, S. *et al.* Microvesicles derived from mesenchymal stem cells enhance survival in a lethal model of acute kidney injury. *PLoS One* **7,** (2012).

29. Bruno, S. *et al.* Mesenchymal stem cell-derived microvesicles protect against acute tubular injury. *J. Am. Soc. Nephrol.* **20,** 1053–1067 (2009).

30. Akyurekli, C. *et al.* A Systematic Review of Preclinical Studies on the Therapeutic Potential of Mesenchymal Stromal Cell-Derived Microvesicles. *Stem Cell Rev. Reports* **11,** 150–160 (2015).

31. Margolis, L. & Sadovsky, Y. The biology of extracellular vesicles: The known unknowns. *PLoS Biol.* **17,** (2019).

32. Shafritz, D. A., Oertel, M., Menthena, A., Nierhoff, D. & Dabeva, M. D. Liver stem cells and prospects for liver reconstitution by transplanted cells. *Hepatology* **43,** (2006).

33. Fausto, N. Liver regeneration and repair: Hepatocytes, progenitor cells, and stem cells. *Hepatology* **39,** 1477–1487 (2004).

34. Herrera, M. B. *et al.* Isolation and Characterization of a Stem Cell Population from Adult Human Liver. *Stem Cells* **24,** 2840–2850 (2006).

35. Fonsato, V. *et al.* Use of a rotary bioartificial liver in the differentiation of human liver stem cells. *Tissue Eng. - Part C Methods* **16,** 123–132 (2010).

36. Navarro-Tableros, V. *et al.* Islet-Like Structures Generated In Vitro from Adult Human Liver Stem Cells Revert Hyperglycemia in Diabetic SCID Mice. *Stem Cell Rev. Reports* **15,** 93–111 (2019).

37. Famulari, E. S. *et al.* Human liver stem cells express UGT1A1 and improve phenotype of immunocompromised Crigler Najjar syndrome type I mice. *Sci. Rep.* **10,** (2020).

38. Herrera, M. B. *et al.* Human liver stem cells improve liver injury in a model of fulminant liver failure. *Hepatology* **57,** 311–319 (2013).

39. Spada, M. *et al.* Intrahepatic Administration of Human Liver Stem Cells in Infants with Inherited

Neonatal-Onset Hyperammonemia: A Phase I Study. *Stem Cell Rev. Reports* **16,** 186–197 (2020).

40. Bruno, S. *et al.* Human Liver-Derived Stem Cells Improve Fibrosis and Inflammation Associated with Nonalcoholic Steatohepatitis. *Stem Cells Int.* **2019,** (2019).

41. Wang, P. *et al.* Promising therapy candidates for liver fibrosis. *Frontiers in Physiology* **7,** (2016).

42. Rockey, D. C. Current and Future Anti-Fibrotic Therapies for Chronic Liver Disease. *Clinics in Liver Disease* **12,** 939–962 (2008).

43. Augustin, H. G. & Koh, G. Y. Organotypic vasculature: From descriptive heterogeneity to functional pathophysiology. *Science* (2017). doi:10.1126/science.aal2379

44. Wisse, E. An electron microscopic study of the fenestrated endothelial lining of rat liver sinusoids. *J. Ultrasructure Res.* (1970). doi:10.1016/S0022-5320(70)90150-4

45. Widmann, J. J. & Fahimi, H. D. Proliferation of mononuclear phagocytes (Kupffer cells) and endothelial cells in regenerating rat liver. A light and electron microscopic cytochemical study. *Am. J. Pathol.* (1975).

46. Ogawa, K., Minase, T., Enomoto, K. & Onoé, T. Ultrastructure of Fenestrated Cells in the Sinusoidal Wall of Rat Liver After Perfusion Fixation. *Tohoku J. Exp. Med.* (1973). doi:10.1620/tjem.110.89

47. Braet, F. & Wisse, E. Structural and functional aspects of liver sinusoidal endothelial cell fenestrae: A review. *Comparative Hepatology* (2002). doi:10.1186/1476-5926-1-1

48. Morsiani, E., Mazzoni, M., Aleotti, A., Gorini, P. & Ricci, D. Increased sinusoidal wall permeability and liver fatty change after two-thirds hepatectomy: An ultrastructural study in the rat. *Hepatology* (1995). doi:10.1016/0270-9139(95)90117-5

49. Fraser, R., Clark, S. A., Day, W. A. & Murray, F. E. M. Nicotine decreases the porosity of the rat liver sieve: A possible mechanism for hypercholesterolaemia. *Br. J. Exp. Pathol.* (1988).

50. Fraser, R., Bosanquet, A. G. & Day, W. A. Filtration of chylomicrons by the liver may influence cholesterol metabolism and atherosclerosis. *Atherosclerosis* (1978). doi:10.1016/0021-9150(78)90001-1

51. Géraud, C. *et al.* Unique cell type-specific junctional complexes in vascular endothelium of human and rat liver sinusoids. *PLoS One* (2012). doi:10.1371/journal.pone.0034206

52. Schaffner, F. & Popper, H. Capillarization of Hepatic Sinusoids in Man. *Gastroenterology* (1963). doi:10.1016/S0016-5085(63)80130-4

53. Martinez-Hernandez, A. & Martinez, J. The role of capillarization in hepatic failure: Studies in carbon tetrachloride-induced cirrhosis. *Hepatology* **14,** 864–874 (1991).

54. Poisson, J. *et al.* Liver sinusoidal endothelial cells: Physiology and role in liver diseases. *Journal of Hepatology* **66,** 212–227 (2017).

55. Xu, M., Wang, X., Zou, Y. & Zhong, Y. Key role of liver sinusoidal endothelial cells in liver fibrosis. *BioScience Trends* **11,** 163–168 (2017).

56. Hammoutene, A. & Rautou, P. E. Role of liver sinusoidal endothelial cells in non-alcoholic fatty liver disease. *Journal of Hepatology* **70,** 1278–1291 (2019).

57. Deleve, L. D. Liver sinusoidal endothelial cells in hepatic fibrosis. *Hepatology* **61,** 1740–1746 (2015).

58. Miyao, M. *et al.* Pivotal role of liver sinusoidal endothelial cells in NAFLD/NASH progression. *Lab.*

Investig. **95,** 1130–1144 (2015).

59. Miyao, M. *et al.* Bile canalicular abnormalities in the early phase of a mouse model of sclerosing cholangitis. *Dig. Liver Dis.* **45,** 216–225 (2013).

60. Lammert, E., Cleaver, O. & Melton, D. Induction of pancreatic differentiation by signals from blood vessels. *Science (80-.).* (2001). doi:10.1126/science.1064344

61. Crivellato, E., Nico, B. & Ribatti, D. Contribution of endothelial cells to organogenesis: A modern reappraisal of an old Aristotelian concept. *Journal of Anatomy* (2007). doi:10.1111/j.1469-7580.2007.00790.x

62. Matsumoto, K., Yoshitomi, H., Rossant, J. & Zaret, K. S. Liver organogenesis promoted by endothelial cells prior to vascular function. *Science (80-.).* (2001). doi:10.1126/science.1063889

63. J., G., P., S. & P., C. Principles of targeting endothelial cell metabolism to treat angiogenesis and endothelial cell dysfunction in disease. *EMBO Molecular Medicine* **6,** 1105–1120 (2014).

64. Knorr, A. *et al.* Nitric oxide-independent activation of soluble guanylate cyclase by BAY 60-2770 in experimental liver fibrosis. *Arzneimittel-Forschung/Drug Res.* **58,** 71–80 (2008).

65. DeLeve, L. D., Wang, X. & Guo, Y. Sinusoidal endothelial cells prevent rat stellate cell activation and promote reversion to quiescence. *Hepatology* **48,** 920–930 (2008).

66. Xie, G. *et al.* Role of differentiation of liver sinusoidal endothelial cells in progression and regression of hepatic fibrosis in rats. *Gastroenterology* **142,** (2012).

67. Zhang, F. *et al.* Curcumin attenuates angiogenesis in liver fibrosis and inhibits angiogenic properties of hepatic stellate cells. *J. Cell. Mol. Med.* **18,** 1392–1406 (2014).

68. Géraud, C. *et al.* GATA4-dependent organ-specific endothelial differentiation controls liver development and embryonic hematopoiesis. *J. Clin. Invest.* (2017). doi:10.1172/JCI90086

69. Duan, J. L. *et al.* Endothelial Notch activation reshapes the angiocrine of sinusoidal endothelia to aggravate liver fibrosis and blunt regeneration in mice. *Hepatology* (2018). doi:10.1002/hep.29834

70. Natarajan, V., Harris, E. N. & Kidambi, S. SECs (Sinusoidal Endothelial Cells), Liver Microenvironment, and Fibrosis. *BioMed Research International* **2017,** (2017).

71. Xu, B. *et al.* Capillarization of hepatic sinusoid by liver endothelial cell-reactive autoantibodies in patients with cirrhosis and chronic hepatitis. *Am. J. Pathol.* **163,** 1275–1289 (2003).

72. McMahan, R. H., Porsche, C. E., Edwards, M. G. & Rosen, H. R. Free fatty acids differentially downregulate chemokines in liver sinusoidal endothelial cells: Insights into non-alcoholic fatty liver disease. *PLoS One* **11,** (2016).

73. Cohen, S. *et al.* Immunogenicity Endothelial Cells Acquire Enhanced In Hepatic Fibrosis, Liver Sinusoidal In Hepatic Fibrosis, Liver Sinusoidal Endothelial Cells Acquire Enhanced Immunogenicity. *J. Immunol.* **185,** 2200–2208 (2010).

74. Connolly, M. K. *et al.* In Hepatic Fibrosis, Liver Sinusoidal Endothelial Cells Acquire Enhanced Immunogenicity. *J. Immunol.* **185,** 2200–2208 (2010).

75. Gracia-Sancho, J. *et al.* Enhanced vasoconstrictor prostanoid production by sinusoidal endothelial cells increases portal perfusion pressure in cirrhotic rat livers. *J. Hepatol.* **47,** 220–227 (2007).

76. May, D. *et al.* A transgenic model for conditional induction and rescue of portal hypertension reveals a role of VEGF-mediated regulation of sinusoidal fenestrations. *PLoS One* **6,** (2011).

77. Rockey, D. C. & Chung, J. J. Reduced nitric oxide production by endothelial cells in cirrhotic rat liver: Endothelial dysfunction in portal hypertension. *Gastroenterology* **114,** 344–351 (1998).

78. Fernández-Iglesias, A. & Gracia-Sancho, J. How to face chronic liver disease: The sinusoidal perspective. *Frontiers in Medicine* **4,** (2017).

79. Eelen, G., De Zeeuw, P., Simons, M. & Carmeliet, P. Endothelial cell metabolism in normal and diseased vasculature. *Circulation Research* **116,** 1231–1244 (2015).

80. Petrillo, S. *et al.* Heme accumulation in endothelial cells impairs angiogenesis by triggering paraptosis. *Cell Death Differ.* **25,** 573–588 (2018).

81. Vandekeere, S. *et al.* Serine Synthesis via PHGDH Is Essential for Heme Production in Endothelial Cells. *Cell Metab.* **28,** 573–587.e13 (2018).

82. Abraham, N. G. *et al.* Heme oxygenase-1 attenuates glucose-mediated cell growth arrest and apoptosis in human microvessel endothelial cells. *Circ. Res.* **93,** 507–514 (2003).

83. Shetty, T., Sishtla, K., Park, B., Repass, M. J. & Corson, T. W. Heme Synthesis Inhibition Blocks Angiogenesis Via Mitochondrial Dysfunction. *SSRN Electron. J.* (2019). doi:10.2139/ssrn.3494377

84. Kus, E. *et al.* LSEC Fenestrae Are Preserved despite Pro-inflammatory Phenotype of Liver Sinusoidal Endothelial Cells in Mice on High Fat Diet. *Front. Physiol.* **10,** (2019).

85. Khan, A. A. & Quigley, J. G. Control of intracellular heme levels: Heme transporters and heme oxygenases. *Biochimica et Biophysica Acta - Molecular Cell Research* **1813,** 668–682 (2011).

86. Faller, M., Matsunaga, M., Yin, S., Loo, J. A. & Guo, F. Heme is involved in microRNA processing. *Nat. Struct. Mol. Biol.* **14,** 23–29 (2007).

87. Imaizumi, T., Kay, S. A. & Schroeder, J. I. CIRCADIAN RHYTHMS: Daily Watch on Metabolism. *Science (80-.).* **318,** 1730–1731 (2007).

88. Wang, S., Publicover, S. & Gu, Y. An oxygen-sensitive mechanism in regulation of epithelial sodium channel. *Proc. Natl. Acad. Sci. U. S. A.* **106,** 2957–2962 (2009).

89. Balla, J. Haem, haem oxygenase and ferritin in vascular endothelial cell injury. *Nephrol. Dial. Transplant.* **18,** 8v–12 (2003).

90. Sensitivity, O. Hypothesis Paper THE HEME SYNTHESIS AND DEGRADATION PATHWAYS : ROLE IN Heme Oxygenase has Both Pro- and Antioxidant Properties. *Science (80-.).* **28,** 289–309 (2000).

91. Halliwell, B. & Gutteridge, J. M. C. Role of free radicals and catalytic metal ions in human disease: An overview. *Methods Enzymol.* **186,** 1–85 (1990).

92. Ponka, P. Tissue-specific regulation of iron metabolism and heme synthesis: Distinct control mechanisms in erythroid cells. *Blood* **89,** 1–25 (1997).

93. Chiabrando, D., Vinchi, F., Fiorito, V., Mercurio, S. & Tolosano, E. Heme in pathophysiology: A matter of scavenging, metabolism and trafficking across cell membranes. *Front. Pharmacol.* **5,** 1–24 (2014).

94. Quigley, J. G. *et al.* Identification of a human heme exporter that is essential for erythropoiesis. *Cell* **118,** 757–766 (2004).

95. Vinchi, F. *et al.* Heme exporter FLVCR1a regulates heme synthesis and degradation and controls activity of cytochromes P450. *Gastroenterology* **146,** 1325–1338 (2014).

96. Chiabrando, D. *et al.* The mitochondrial heme exporter FLVCR1b mediates erythroid differentiation. *J. Clin. Invest.* **122,** 4569–4579 (2012).

97. Keel, S. B. *et al.* A heme export protein is required for red blood cell differentiation and iron homeostasis. *Science (80-.).* **319,** 825–828 (2008).

98. Tailor, C. S., Willett, B. J. & Kabat, D. A Putative Cell Surface Receptor for Anemia-Inducing Feline Leukemia Virus Subgroup C Is a Member of a Transporter Superfamily. *J. Virol.* **73,** 6500–6505 (1999).

99. Quigley, J. G. *et al.* Cloning of the cellular receptor for feline leukemia virus subgroup C (FeLV-C), a retrovirus that induces red cell aplasia. *Blood* **95,** 1093–1099 (2000).

100. Fiorito, V., Forni, M., Silengo, L., Altruda, F. & Tolosano, E. Crucial role of FLVCR1a in the maintenance of intestinal heme homeostasis. *Antioxidants Redox Signal.* **23,** 1410–1423 (2015).

101. Chiabrando, D. *et al.* Mutations in the Heme Exporter FLVCR1 Cause Sensory Neurodegeneration with Loss of Pain Perception. *PLoS Genet.* **12,** (2016).

102. Rajadhyaksha, A. M. *et al.* Mutations in FLVCR1 cause posterior column ataxia and retinitis pigmentosa. *Am. J. Hum. Genet.* **87,** 643–654 (2010).

103. Bertino, F. *et al.* Heme and sensory neuropathy: Insights from novel mutations in the heme exporter feline leukemia virus subgroup C receptor 1. *Pain* **160,** 2766–2775 (2019).

104. Castori, M. *et al.* Posterior column ataxia with retinitis pigmentosa coexisting with sensory-autonomic neuropathy and leukemia due to the homozygous p.Pro221Ser FLVCR1 mutation. *Am. J. Med. Genet. Part B Neuropsychiatr. Genet.* **174,** 732–739 (2017).

105. Fickert, P. *et al.* A new xenobiotic-induced mouse model of sclerosing cholangitis and biliary fibrosis. *Am. J. Pathol.* **171,** 525–536 (2007).

106. Fickert, P. *et al.* Characterization of animal models for primary sclerosing cholangitis (PSC). *Journal of Hepatology* **60,** 1290–1303 (2014).

107. Friedman, S. L. Mechanisms of Hepatic Fibrogenesis. *Gastroenterology* **134,** 1655–1669 (2008).

108. Hemmann, S., Graf, J., Roderfeld, M. & Roeb, E. Expression of MMPs and TIMPs in liver fibrosis - a systematic review with special emphasis on anti-fibrotic strategies. *J. Hepatol.* **46,** 955–975 (2007).

109. Clerbaux, L.-A. *et al.* Relevance of the CDE and DDC Mouse Models to Study Ductular Reaction in Chronic Human Liver Diseases. in *Experimental Animal Models of Human Diseases - An Effective Therapeutic Strategy* (2018). doi:10.5772/intechopen.69533

110. Iredale, J. P. Models of liver fibrosis: Exploring the dynamic nature of inflammation and repair in a solid organ. *Journal of Clinical Investigation* **117,** 539–548 (2007).

111. Tasci, Ii. *et al.* Rat liver fibrosis regresses better with pegylated interferon α2b and ursodeoxycholic acid treatments than spontaneous recovery. *Liver Int.* **26,** 261–268 (2006).

112. Constandinou, C., Henderson, N. & Iredale, J. P. Modeling liver fibrosis in rodents. *Methods Mol. Med.* **117,** 237–250 (2005).

113. Di Vinicius, I., Baptista, A. P., Barbosa, A. A. & Andrade, Z. A. Morphological signs of cirrhosis regression. Experimental observations on carbon tetrachloride-induced liver cirrhosis of rats. *Pathol. Res. Pract.* **201,** 449–456 (2005).

114. Pérez-Tamayo, R. Cirrhosis of the liver: a reversible disease? *Pathology Annual* **14 Pt 2,** 183–213 (1979).

115. Iredale, J. P. *et al.* Mechanisms of spontaneous resolution of rat liver fibrosis: Hepatic stellate cell apoptosis and reduced hepatic expression of metalloproteinase inhibitors. *J. Clin. Invest.* **102,**

538–549 (1998).

116. Maros, T., Seres-Sturm, L., Lakatos, O. & Blazsek, V. Spontaneous reversibility of advanced toxic liver cirrhosis. *Acta Morphol. Acad. Sci. Hung.* **23,** 293–302 (1975).

117. Kholia, S. *et al.* Mesenchymal Stem Cell Derived Extracellular Vesicles Ameliorate Kidney Injury in Aristolochic Acid Nephropathy. *Front. Cell Dev. Biol.* **8,** (2020).

118. Brossa, A. *et al.* Extracellular vesicles from human liver stem cells inhibit renal cancer stem cell-derived tumor growth in vitro and in vivo . *Int. J. Cancer* (2020). doi:10.1002/ijc.32925

119. Grange, C. *et al.* Stem cell-derived extracellular vesicles inhibit and revert fibrosis progression in a mouse model of diabetic nephropathy. *Sci. Rep.* **9,** (2019).

120. Bruno, S. *et al.* HLSC-Derived Extracellular Vesicles Attenuate Liver Fibrosis and Inflammation in a Murine Model of Non-alcoholic Steatohepatitis. *Mol. Ther.* **28,** 479–489 (2020).

121. Grange, C. *et al.* Biodistribution of mesenchymal stem cell-derived extracellular vesicles in a model of acute kidney injury monitored by optical imaging. *Int. J. Mol. Med.* **33,** 1055–1063 (2014).

122. Nolan, D. J. *et al.* Molecular Signatures of Tissue-Specific Microvascular Endothelial Cell Heterogeneity in Organ Maintenance and Regeneration. *Dev. Cell* (2013). doi:10.1016/j.devcel.2013.06.017

123. Tai, Y. *et al.* SK-Hep1: not hepatocellular carcinoma cells but a cell model for liver sinusoidal endothelial cells. *Int. J. Clin. Exp. Pathol.* **11,** 2931–2938 (2018).

124. Rodriguez-Vita, J. & Morales-Ruiz, M. Down the liver sinusoidal endothelial cell (LSEC) hole. Is there a role for lipid rafts in LSEC fenestration? *Hepatology* **57,** 1272–1274 (2013).

125. Svistounov, D. *et al.* The Relationship between Fenestrations, Sieve Plates and Rafts in Liver Sinusoidal Endothelial Cells. *PLoS One* **7,** (2012).

126. Zapotoczny, B. *et al.* Atomic Force Microscopy Reveals the Dynamic Morphology of Fenestrations in Live Liver Sinusoidal Endothelial Cells. *Sci. Rep.* **7,** (2017).

127. Owen, O. E., Kalhan, S. C. & Hanson, R. W. The key role of anaplerosis and cataplerosis for citric acid cycle function. *Journal of Biological Chemistry* **277,** 30409–30412 (2002).

128. Sachar, M., Anderson, K. E. & Ma, X. Protoporphyrin IX: The good, the bad, and the ugly. *J. Pharmacol. Exp. Ther.* **356,** 267–275 (2016).

129. Ikushiro, H. *et al.* Heme-dependent Inactivation of 5-Aminolevulinate Synthase from Caulobacter crescentus. *Sci. Rep.* **8,** (2018).

130. Russell, A. E. *et al.* Biological membranes in EV biogenesis, stability, uptake, and cargo transfer: an ISEV position paper arising from the ISEV membranes and EVs workshop. in *Journal of Extracellular Vesicles* **8,** (2019).

131. Allijn, I. E. *et al.* Liposome encapsulated berberine treatment attenuates cardiac dysfunction after myocardial infarction. *J. Control. Release* **247,** 127–133 (2017).

132. Van Beers, B. E. *et al.* Capillarization of the sinusoids in liver fibrosis: Noninvasive assessment with contrast-enhanced MRI in the rabbit. *Magn. Reson. Med.* **49,** 692–699 (2003).

133. Böttger, R. *et al.* Lipid-based nanoparticle technologies for liver targeting. *Advanced Drug Delivery Reviews* **154–155,** 79–101 (2020).

134. Winkler, M. *et al.* Endothelial GATA4 controls liver fibrosis and regeneration by preventing a

pathogenic switch in angiocrine signaling. *J. Hepatol.* **74,** 380–393 (2021).

135. Nayor, M. & Vasan, R. S. Recent update to the us cholesterol treatment guidelines: A comparison with international guidelines. *Circulation* **133,** 1795–1806 (2016).

136. Pose, E., Trebicka, J., Mookerjee, R. P., Angeli, P. & Ginès, P. Statins: Old drugs as new therapy for liver diseases? *Journal of Hepatology* **70,** 194–202 (2019).

137. Marrone, G. *et al.* The transcription factor KLF2 mediates hepatic endothelial protection and paracrine endothelial-stellate cell deactivation induced by statins. *J. Hepatol.* **58,** 98–103 (2013).

138. Marrone, G. *et al.* KLF2 exerts antifibrotic and vasoprotective effects in cirrhotic rat livers: Behind the molecular mechanisms of statins. *Gut* **64,** 1434–1443 (2015).

139. Riganti, C. *et al.* Atorvastatin modulates anti-proliferative and pro-proliferative signals in Her2/neu-positive mammary cancer. *Biochem. Pharmacol.* **82,** 1079–1089 (2011).

140. Trebicka, J. & Schierwagen, R. Statins, Rho GTPases and KLF2: New mechanistic insight into liver fibrosis and portal hypertension. *Gut* **64,** 1349–1350 (2015).

141. Bravo, M. *et al.* Restoration of liver sinusoidal cell phenotypes by statins improves portal hypertension and histology in rats with NASH. *Sci. Rep.* **9,** (2019).

142. Sinclair, P. R., Gorman, N. & Jacobs, J. M. Measurement of Heme Concentration. *Curr. Protoc. Toxicol.* **0,** 8.3.1-8.3.7 (1999).

143. Schilling, R., Geserick, P. & Leverkus, M. Characterization of the ripoptosome and its components: Implications for anti-inflammatory and cancer therapy. in *Methods in Enzymology* **545,** 83–102 (2014).

144. Pinzõn-Daza, M. L. *et al.* The association of statins plus LDL receptor-targeted liposome-encapsulated doxorubicin increases in vitro drug delivery across blood-brain barrier cells. *Br. J. Pharmacol.* **167,** 1431–1447 (2012).

145. Chen, Y., Tang, Y., Long, W. & Zhang, C. Stem Cell-Released Microvesicles and Exosomes as Novel Biomarkers and Treatments of Diseases. *Stem Cells International* **2016,** (2016).

146. Petrillo, S., Manco, M., Altruda, F., Fagoonee, S. & Tolosano, E. Liver Sinusoidal Endothelial Cells at the crossroad of Iron overload and Liver Fibrosis. *Antioxid. Redox Signal.* (2020). doi:10.1089/ars.2020.8168